Chemistry

porcelanites and cherts which together with organic matter and phosphorite, constitute the so-called P-C-Si trilogy (Bentor 1980). Many other phases occur in phosphorites, notably dolomite, glauconite, sulphides (pyrite), sulphates (gypsum), clinoptilolite, clay minerals (illite, kaolinite, palygorskite, smectites) and organic matter. Clearly, the proportions, distributions, grain sizes and textural characteristics of such accessory phases have important implications for the extraction and beneficiation of a deposit.

Chemistry

Francolite chemistry may be affected by a number of factors, including: (1) kinetic effects due to the rate of formation; (2) thermodynamic factors; (3) precipitation from solutions of different composition due to secular variation in seawater or evolving porewater chemistry; (4) mechanism of formation, such as differences resulting from precipitation directly from solution or via dissolution and replacement of a pre-existing mineral (most commonly calcite), or bacterially mediated versus 'inorganic' precipitation; (5) post-precipitation burial diagenetic or metamorphic alteration; (6) weathering. The relative importance of these factors is still not well-constrained, but their significance will become apparent in the ensuing discussion.

Over the last decade, new information concerning the geochemical processes which lead to francolite precipitation and the formation of phosphorites has been derived from three main sources: (1) pore-water and solid-phase geochemical studies of sediments from modern phosphogenic areas, particularly the Mexican, Peru and East Australian shelves (Froelich et al. 1983; Jahnke et al. 1983; Glenn et al. 1988, 1994a; Van Cappellen & Berner 1988; Glenn 1990a; Heggie et al. 1990; O'Brien et al. 1990); (2) oxygen, carbon and sulphur stable-isotope studies of modern and ancient phosphorites (see Kolodny & Luz 1992a for a recent review); (3) geochemical and mineralogical data, and modelling of inorganic and bacterially-mediated apatite precipitation under experimental conditions (Lucas & Prévôt 1981, 1984, 1985; Jahnke 1984; Prévôt & Lucas 1986; Van Cappellen & Berner 1988, 1991; Prévôt et al. 1989).

Major elements

The major-element geochemistry of unaltered francolites display surprisingly little variation; unweathered Cenozoic francolites (McArthur 1978a, 1980, 1985, pers. comm. 1994) contain 32% P_2O_5, 52% CaO, 4% F, and typically include (%): 1.2 ± 0.2 Na; 0.25 ± 0.02 Sr; 0.36 ± 0.03 Mg; 6.3 ± 0.3 CO_2; 2.7 ± 0.3 SO_4. In general, the level of substitution shown by the mineral decreases progressively with increasing age, burial diagenesis and/or weathering, which promote a transition towards unsubstituted fluorapatite [$Ca_{10}(PO_4)_6F_2$] compositions. With the onset of greenschist facies metamorphism, hydroxyfluorapatites may develop (Da Rocha Araujo et al. 1992; Girard et al. 1993). Subsequently, under extreme weathering conditions, Fe- and Al-phosphate minerals such as crandallite, millisite, wavellite and strengite commonly form (Zanin 1968; Altschuler 1973; Lucas et al. 1980; Schwab & Oliveira 1981; Flicoteaux 1982; Flicoteaux & Lucas 1984; Bonnot-Courtois & Flicoteaux 1989).

The major-element chemistry of phosphorites reflects both the composition of francolite and that of accessory minerals. Consequently, SiO_2 for example, is highest in quartz-

rich deposits, such as the Miocene phosphorites of the SE United States. This is exemplified in Table 2, which shows the major-element composition of three phosphorite ore concentrates: Western Phosphate Rock from the US Permian Phosphoria Formation (NIST 694); Moroccan Phosphate Rock (BCR 32, Eocene); Florida Phosphate Rock (NIST 120c, Miocene). The much higher proportions of quartz and clay minerals in the Florida sample are clearly indicated by elevated levels of SiO_2 and, to a lesser extent, Al_2O_3.

Carbonate and fluorine substitution

The vast majority of unweathered seafloor phosphorites have francolite-CO_2 contents (generally determined using the XRD-method of Gulbrandsen 1970; see Schuffert et al. 1990 for a revised equation) of around 6.3%, close to the maximum substitution allowable by the mineral structure (McClellan & Lehr 1969; McClellan 1980; Jahnke 1984; McClellan & van Kauwenbergh 1990). However, significant variation in francolite-CO_2 contents have been observed in many ancient and some modern phosphorites. The cause of this variation has been the focus of considerable debate.

Gulbrandsen (1970), studying the Phosphoria Formation of Idaho and Wyoming, noted that the average CO_2-contents of francolites taken from carbonate-phosphorite deposits in central Wyoming are moderately high (3.4% CO_2), but they decrease progressively westwards towards SE Idaho with the transition to mudstone-chert-phosphorite facies (1.2%). He suggested that this systematic variation related to primary differences in dep-

Tab. 2. Major-element composition of phosphorite ore concentrates

Element	NIST 120c Western	BCR 32 Moroccan	NIST 694 Florida
		(%)	
SiO_2	5.5	2.09	11.2
TiO_2	0.103	0.0285	0.11
Al_2O_3	1.30	0.55	1.8
Fe_2O_3	1.08	0.231	0.79
MnO	0.027	0.0024	0.0116
MgO	0.32	0.403	0.33
CaO	48.02	51.76	43.6
Na_2O	0.52	n.d.	0.86
K_2O	0.147	n.d.	0.51
P_2O_5	33.34	32.98	30.2
CO_2	3.27	5.10	n.d.
F	3.82	4.04	3.20
SO_3	0.92	1.84	n.d.

Data from Potts et al. 1992b; BCR = Community Bureau of Reference, Belgium; NIST = National Institute of Standards and Technology, USA; total Fe expressed as Fe_2O_3; n.d. = not determined

ositional environments, predominantly temperature differences causing vary CO_2-saturation in the water column. Later, McArthur (1985) expressed the view that this regional variation could be ascribed solely to late diagenetic effects having caused greater loss of structural carbonate from more deeply buried western sites.

There is no doubt that burial diagenesis, metamorphism and weathering generally cause the loss of CO_2 and other constituents from the francolite structure (Jacob et al. 1933; Bliskovskiy 1976; Gusev et al. 1976, Zanin & Krivoputskaya 1976; Matthews & Nathan 1977; Lucas et al. 1980; McArthur 1980, 1985; McClellan 1980; Zanin et al. 1985; McClellan & Saavedra 1986; Panczer et al. 1989; Da Rocha Araujo et al. 1992). During deep-burial (km-scale), an inverse relationship between CO_2-content and temperature develops (Kastner et al. 1990), although later stage, CO_2-rich secondary carbonate-hydroxyfluorapatites have been reported (Da Rocha Araujo et al. 1992) from deposits affected by low-grade metamorphism. In the case of Phosphoria Formation francolites, a strong correlation between SO_4^{3-} concentration and $\delta^{34}S$, and the consistency of $\delta^{18}O$ data (Piper & Kolodny 1987; see below for further discussion of isotopic data), both suggest that these isotopes reflect initial conditions of deposition, so the degree of alteration cannot be high. Furthermore, Upper Cretaceous-Palaeogene phosphorites from Israel (Nathan et al. 1990) display similar variations in structural CO_2 to the Phosphoria Formation, with francolites from well-oxygenated carbonate-rich depositional environments exhibiting greater substitution (5.5% CO_2) than those from granular phosphorites associated with anoxic facies (3.7%) in the same region. Differential weathering does not appear to be responsible for these trends, pointing to a primary geochemical difference between the areas.

Namibian seafloor phosphorites exhibit a range of phosphate-CO_2 contents from 1.4% in poorly consolidated nodules to 4.2% in indurated nodules and pellets (Romankevich & Baturin 1972; Price & Calvert 1978). This may be due to the fact that these young phosphorites include varying amounts of a francolite precursor phase (see below) which contains little or no structural CO_2. Another potential cause of such variation has been identified from studies of Holocene phosphorites off Peru (Glenn et al. 1988; Glenn 1990a), which contain between 2.1 and 6.0% CO_2. A correlation between lighter carbon stable-isotope compositions (more negative $\delta^{13}C$; see below) with increasing CO_2 contents in francolites, led Glenn and co-workers to conclude that carbonate substitution depends mainly on the carbonate alkalinity (and hence CO_3^{2-} concentrations) of the pore waters, which increases progressively with depth in the sediment. Rather surprisingly, pH is relatively constant despite the rapid generation of metabolic CO_2, because pH is buffered by ammonia production and increases in total alkalinity. The constancy of pH observed in the Peru margin sediments is important, not least because HCO_3/CO_3^{2-} ratios are affected considerably by pH, and are not just dependant on total alkalinity. Indeed, a relatively small fall in pH may reverse the relationship seen between total alkalinity and CO_3^{2-}.

In the organic-rich (up to 20% C_{org}) sediments of the Peru-Chile and Mexican margins, francolite formation is restricted to within 5– 20 cm of the sediment/water interface (Fig. 1, 2), because precipitation ceases at the high carbonate alkalinities which develop rapidly in deeper sediments. Precipitation is probably limited by the ability of the mineral to incorporate carbonate, so elsewhere, in less organic-rich sediments with shallower alkalinity gradients, francolite may form at greater depths. In one Peru margin nodule,

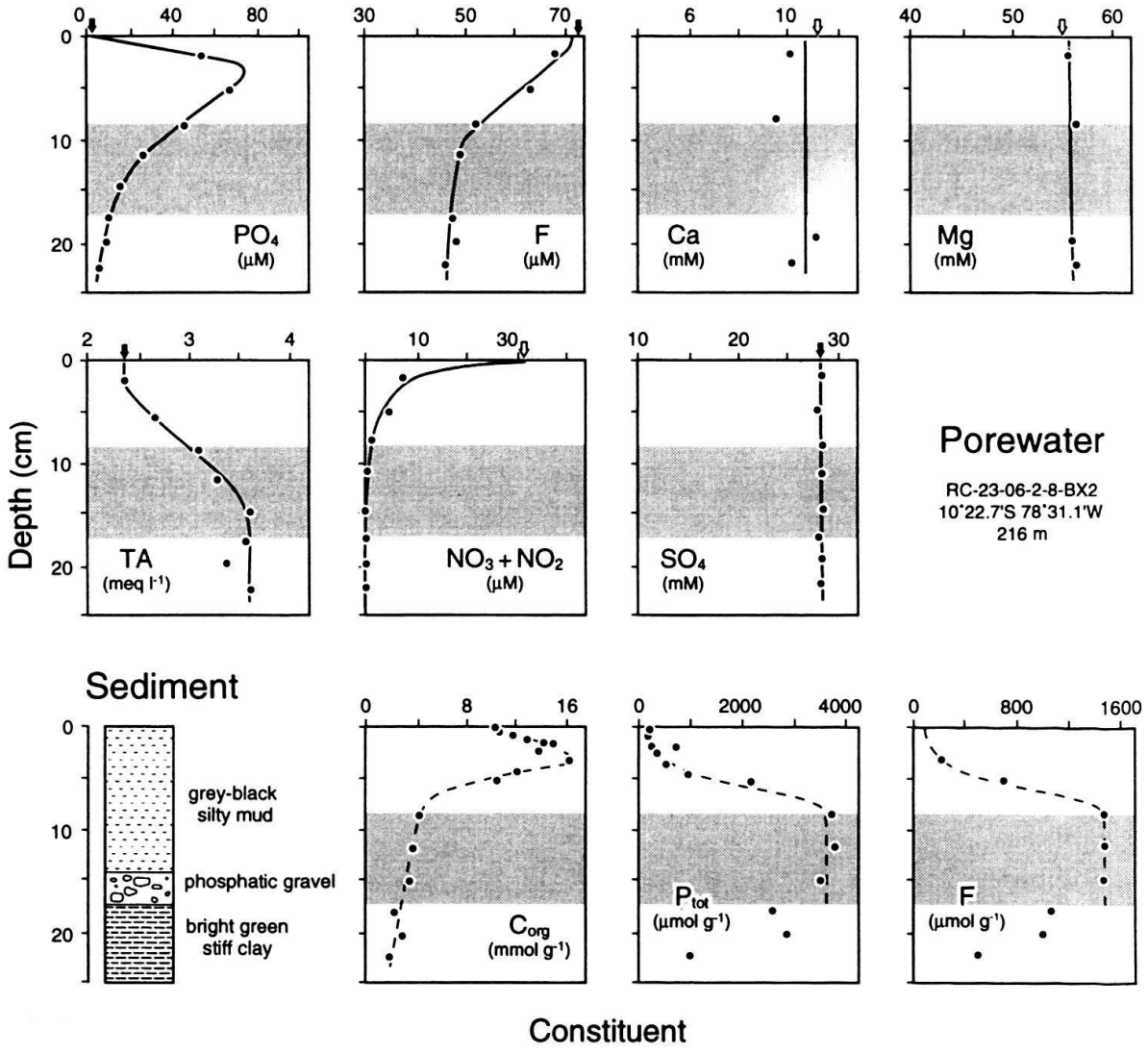

Fig. 1. Porewater and solid-phase geochemistry for slowly accumulating (1.7 cm kyr^{-1}) sediments in a modern upwelling area on the Peru continental margin, 230 km NW of Lima. Black arrows at the tops of graphs are measured seawater values; white arrows are estimated concentrations. The porewater PO_4 profile indicates production of dissolved phosphate in the uppermost 10 cm of sediment and active phosphate precipitation around and below that depth (stippled areas). Fluorine decreases progressively below the sediment/water interface, suggesting that it is supplied to the precipitating phosphate largely by diffusion from seawater. Calcium and Mg contents do not differ significantly from those in seawater. Nitrate, SO_4 and total alkalinity (TA) profiles demonstrate that phosphate is precipitating in suboxic (i.e. NO_3^-, NO_2^-reducing, non-sulphidic), mildly alkaline conditions. Significant levels of Mn, Fe or H_2S were not detected. Solid-phase geochemical profiles (dashed lines) are consistent with rapid degradation of organic matter (declining C_{org} contents) and precipitation of phosphate (increasing total P and F) below 5 cm. Biogenic opal is virtually absent in this core. Precipitation is apparently occurring both within and above a bed of phosphorite clasts and grains (data from: Froelich et al. 1988; Glenn 1990a).

increasing CO_2 substitution could be correlated with decreasing growth rate. This may simply reflect the increasing solubility of more carbonate-substituted apatite (Chien & Black 1976; Jahnke 1984), but it may also point to a kinetic effect limiting substitution in rapidly precipitated francolites.

The availability of dissolved fluoride undoubtedly plays an important role in regulating the precipitation of francolite (Froelich et al. 1983, 1988; Jahnke et al. 1983; Van Cappellen & Berner 1988; Ruttenberg & Berner 1993). As with structural CO_2, the F contents of francolites formed in organic-poor glauconitic carbonate sediments of low productivity areas such as the East Australian Shelf and Agulhas Bank off South Africa, are significantly higher than those typical of francolites from organic-rich muds from high productivity areas off Namibia, Peru and Mexico (Romankevich & Baturin 1972; Price & Calvert 1978; O'Brien et al. 1990). Average F/P_2O_5 ratios of phosphorites from carbonate-dominated areas are close to those occurring in 'ideal' francolite; in addition to containing less CO_2, those associated with more organic-rich sediments typically contain up to one-third less F. This broad correlation between carbonate and fluoride contents is readily explained by the substitution of $CO_3 \cdot F^{3-}$ for PO_4^{3-} in francolite (Borneman-Starinkevich & Belov 1940, 1953; Smith & Lehr 1966; McClellan & Lehr 1969; Price & Calvert 1978; Bacquet et al. 1980; McArthur 1990). Indeed, the relationship appears to be linear in unweathered francolites (McArthur 1990 Fig. 1), scatter being introduced by alteration causing the preferential loss of CO_2 (and OH^- ?) from the mineral.

It is evident that the amount of CO_2 and F substitution in francolite does indeed vary with depositional/early diagenetic environment, and it is speculated that high carbonate alkalinities and slow precipitation rates favour the incorporation of both constituents. In general, carbonate-associated phosphorites contain more structural CO_2 and F than those forming in organic-rich mudrocks. This may be due to differences in kinetics, 'replacement' being much slower than 'direct' precipitation. However, both components may be lost during deep-burial diagenesis, metamorphism and/or weathering which can substantially modify the primary signature.

Magnesium incorporation and inhibition effects

In contrast to CO_3 and F, unaltered francolites display very little variation in their Mg, Na, Sr and SO_4 contents (McArthur 1978a, 1985). Unweathered francolites typically contain around 3600 $\mu g\ g^{-1}$ Mg, but early experimental work (Bachra et al. 1965; Martens & Harris 1970; Atlas 1975; Atlas & Pytkowicz 1977; Nathan & Lucas 1976; Savenko 1978) clearly demonstrated that apatite precipitation is inhibited by Mg concentrations present in seawater and marine porewaters (1300 $\mu g\ g^{-1}$). This effect has been explained as the result of distortion of the embryonic apatite lattice by Mg^{2+} ions replacing Ca^{2+} promoting a wagnerite rather than apatite structure, a distortion strong enough to inhibit further crystal growth. Recent experimental data (Van Cappellen & Berner 1991), however, indicate that it is more likely to be caused by blocking of Ca sites by hydrated Mg-complexes.

Burnett (1977), amongst others, has argued that the removal of Mg by the formation of authigenic minerals such as dolomite or palygorskite must be necessary for francolite precipitation. However, many phosphorites contain no significant Mg-bearing phase, while dolomite may itself be replaced by apatite (Cook pers. comm. 1994), suggesting that Mg removal is not essential. Magnesium inhibition has been shown to be pH dependant (Nathan & Lucas 1976; Van Cappellen & Berner, 1991) with an increase in growth rate kinetics at pH 7 compared with pH 8, despite the thermodynamic disadvantage of increasing apatite solubility with decreasing pH (Atlas 1975; Atlas & Pytkowicz 1977).

Porewater data from modern phosphogenic sediments (Fig. 1, 2) show no depletion in Mg^{2+} below seawater values (Baturin, 1978; Jahnke et al. 1983; Froelich et al. 1988). Furthermore, although low pH of around 7.5 have been reported from both Namibian and Peru-Chile sediments (Baturin et al. 1970; Manheim et al. 1975), no relationship between low pH and sites of apatite precipitation has been established (Jahnke et al. 1983; Glenn et al. 1988).

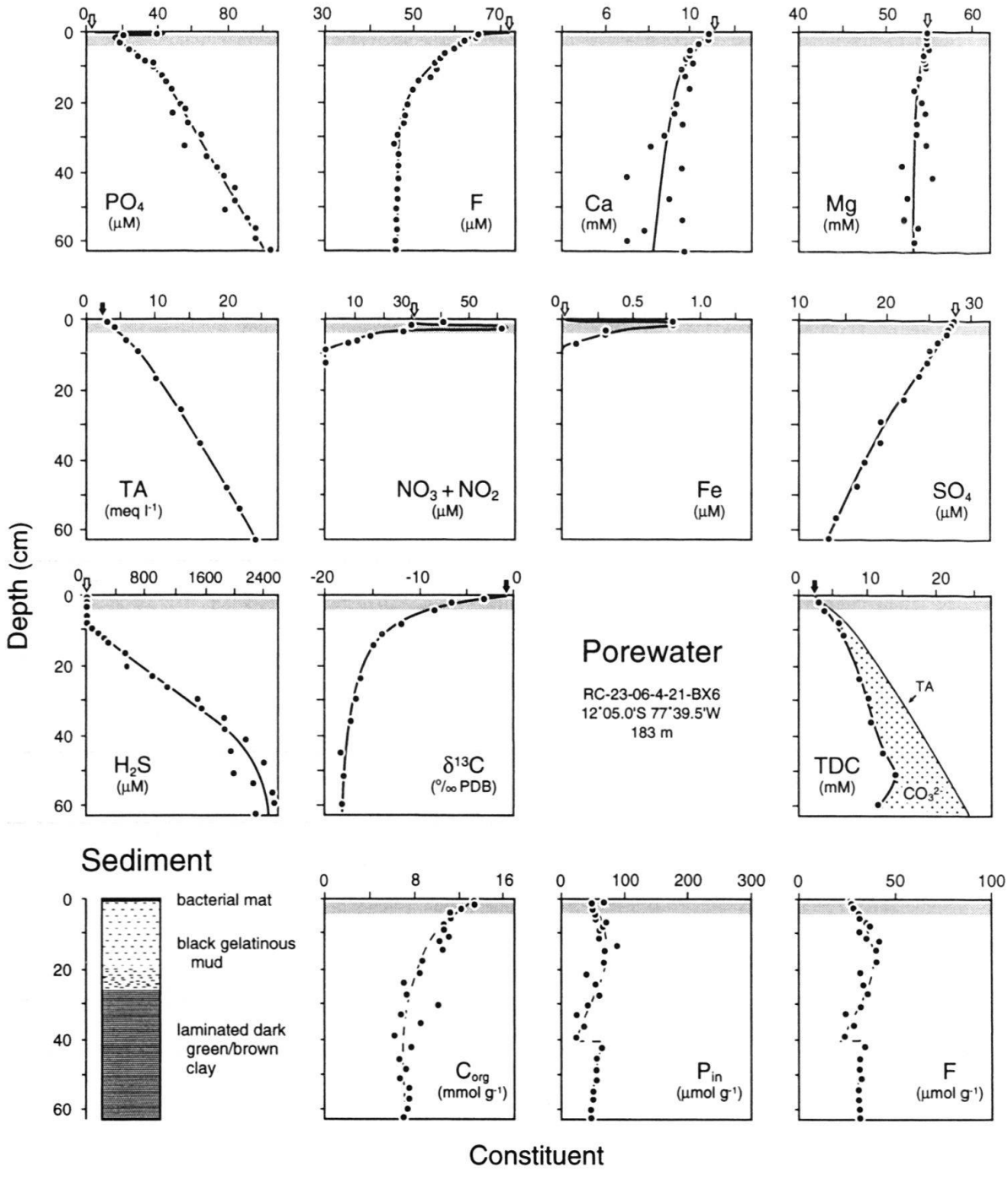

Recent work has resolved some of these apparent inconsistencies. It has been demonstrated experimentally that apatite may precipitate from seawater via an amorphous, F-poor precursor such as struvite ($NH_4MgPO_4 \cdot 6H_2O$; Malone & Towe 1970; Lucas & Prévôt 1985; Prévôt et al. 1989), amorphous calcium magnesium phosphate (ACMP; Froelich et al. 1988; Krajewski et al. 1994) and/or octacalcium phosphate (OCP_p, $Ca_4H(PO_4)_3 \cdot \chi H_2O$; Van Cappellen & Berner 1991). A precursor appears to be involved whether precipitation occurs directly from seawater or via the dissolution and 'replacement' of an existing mineral, such as calcite.

Support for a precursor in modern phosphogenic environments is provided by pore-water data from the Peru margin which display uncoupled PO_4 and F removal (Froelich et al. 1988). Once precipitated, the metastable precursor gradually dissolves and acts as a substrate for apatite precipitation. Thus seawater is probably saturated with respect to francolite but the kinetics are too slow to allow its precipitation. The opposite is true of precursor phases which precipitate rapidly but only at elevated PO_4 levels. Supersaturation with respect to the precursor most likely occurs intermittently within the interfacial pore-water phosphate maximum that characterises many phosphogenic areas (Fig. 1, 2; Krajewski et al. 1984 Fig. 8). The mechanism producing this maximum is not well understood, but may be related to the redox-sensitive uptake and release of phosphorus by microbial communities proliferating in the top sediment, the metabolic activity of sulphide-oxidising or other bacteria, suboxic bacterial degradation of organic matter, the dissolution of fish debris, and/or iron-redox cycling (see below). Organic compounds may also be instrumental in catalysing the precipitation process.

Temporary supersaturation will cause precipitation of a phosphate precursor which, once seeded, will promote apatite growth at much lower PO_4 concentrations. Nonetheless, experimental studies consistently demonstrate that such apatites display poor crystallinity, and 'ageing' on a time scale of 10–100 years (Gulbrandsen et al. 1984) seems to be necessary to produce a typical francolite structure. Furthermore, growth kinetics

---

Fig. 2. Porewater and solid-phase geochemistry for rapidly accumulating (230 cm kyr^{-1}) sediments in a modern upwelling area on the Peru continental margin, 60 km west of Lima. Black arrows at the tops of graphs are measured seawater values; white arrows are estimated concentrations. Porewater profiles indicate intense anoxic diagenesis below 10 cm, with high rates of sulphate reduction (SO_4 depletion, evolution of H_2S). Disequilibrium suboxic nitrate and Fe are present in the upper well-mixed 5–10 cm. An interfacial high in PO_4, combined with a marked minimum in the porewater profile around the base of the bacterial mat at 3–4 cm, suggest active phosphate regeneration above and precipitation within this interval (stippled area). Fluorine is sourced largely by diffusion from seawater. Calcium and Mg contents do not differ significantly from those in seawater at this depth. Below 5 cm, intense sulphate reduction produces exponential downward increases in total alkalinity (TA), total dissolved carbon (TDC), and by difference, total dissolved carbonate-ion (CO_3^{2-}) concentrations. Porewaters rapidly develop highly depleted carbon stable-isotope signatures, down to –18‰ $\delta^{13}C$, indicating domination of the dissolved carbon reservoir by degrading organic matter. Phosphate precipitation is confined to the uppermost 5 cm of the sediment column and may be limited, at least in part, by high carbonate-ion concentrations preventing growth at greater depths (see text for discussion). Solid-phase C_{org} data demonstrate progressive regeneration of organic matter in the sediment under both suboxic and anoxic conditions. Variations in solid-phase inorganic phosphorus (P_{in}) and F are caused by fluctuations in biogenic silica, which constitutes a major component of the sediment at this site. Phosphate grains were not identified in the core, the high sedimentation rate precluding the development of a phosphorite deposit (data from: Froelich et al. 1988; Glenn et al. 1988; Glenn 1990a).

initially limit crystal sizes to the order of 0.1–10 μm (Van Cappellen & Berner 1991). The multi-phase aspect of francolite precipitation, in particular, makes the experimental determination of thermodynamic and kinetic factors extremely problematic.

It must be concluded that although Mg depletion is helpful for the formation of crystalline apatite because it shortens the time required for crystallisation, it is not necessary and is probably uncommon during the formation of phosphorites.

Strontium

Unweathered francolites typically contain around 2500 $\mu g\ g^{-1}$ of Sr (McArthur 1978a, 1985), although "average" phosphorite (Altschuler 1980) has only 750 $\mu g\ g^{-1}$. Lucas et al. (1990) demonstrated that, under experimental conditions, the Sr content of apatite is largely thermodynamically controlled with varying compositions reflecting equilibrium precipitation from fluids of varying Sr content. The small variation in Sr and other major elements displayed by marine francolites probably results from the relatively constant composition of seawater (~7.6 $\mu g\ g^{-1}$ Sr) and shallow porewaters, and the absence of significant kinetic effects. Strontium isotope data (see below) confirm that although francolites undergo negligible diagenetic exchange of Sr, weathering promotes rapid Sr loss (Bliskovskiy et al. 1967; McArthur 1978a, 1985; Panczer et al. 1989); Na and SO_4 appear to be less mobile but are also lost.

McArthur et al. (1988) observed from their study of western South African phosphorites that although modern francolites all have consistent Sr/Ca ratios, significant differences could be identified in age groups of Tertiary samples. Graham et al. (1982), based on geochemical variation in the tests of Cenozoic planktonic foraminifera, suggested that the Sr/Ca ratio of seawater varied significantly during the Tertiary. This offers the possibility that francolite major-element geochemistry may provide information on secular variation in seawater elemental, as well as isotopic, composition. Unfortunately, to date, subsequent workers have been unable to duplicate Graham et al.'s (1982) curve, and published data for phosphorites are insufficient to test the hypothesis.

Iron geochemistry – a key to phosphogenesis?

Francolite incorporates little Fe in its structure, and dissolved Fe-concentrations in oxic seawater are also very low, typically less than 40 $pg\ g^{-1}$. However, iron oxyhydroxide-rich Neogene phosphorite nodules occur on a number of present-day continental shelves, including the Agulhas Bank, South Africa (Parker 1975; Parker & Siesser 1972), Danois Bank, Spain (Lucas et al. 1978), East Australian Shelf (Marshall & Cook 1980; O'Brien & Veeh 1980; O'Brien et al. 1986, 1987, 1990), and off Morocco (McArthur 1978b; Summerhayes & McArthur 1990). A close relationship between iron minerals and francolite occurs in many modern and ancient phosphorites (Glenn 1990b; Glenn et al. 1994a, b), but glauconite is generally the dominant iron mineral present, forming a characteristic greensand – nodular phosphorite facies association. Most Neogene Fe-rich nodules occur in glauconitic sands.

The strong positive correlation between Fe and P in Quaternary phosphorite-bearing sediments from the East Australian Shelf (Heggie et al. 1990; O'Brien et al. 1990), together with sedimentological, petrographic and porewater geochemical data, have led to the realisation that the diagenetic behaviour of the two elements may be closely linked.

The iron-redox model suggests that ferric oxyhydroxides scavenge F from seawater, and PO_4^{3-} released from organic matter by microbial decomposition under oxic and suboxic conditions within the top few cm of sediment (Fig. 3). These FeOOH particles are subsequently transferred deeper into the suboxic zone by burial and sediment-mixing processes where they dissolve and both F and PO_4^{3-} are released. Some of these are then taken up by apatite precipitation, much of the remainder diffusing upwards to be refixed by ferric oxyhydroxides in the oxic layer to become available for further recycling. Glauconite formation may be linked to the same process (Froelich et al. 1988; Carson & Crowley 1993), with a proportion of the porewater Fe^{2+} and $Si(OH)_4$ derived from the dissolution of biogenic opal, together with K^+ and Mg^{2+} ions diffusing into the sediment from seawater, reacting with the aluminosilicate fraction to precipitate glauconite.

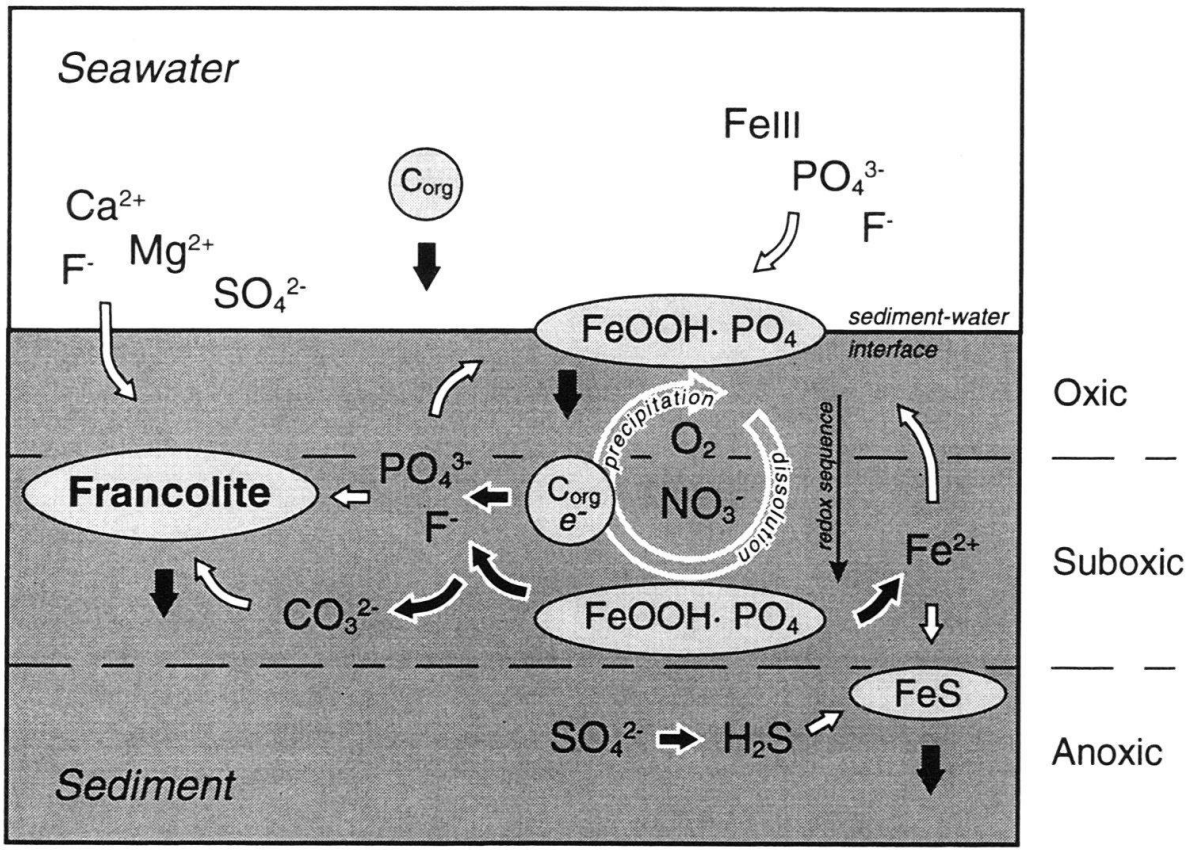

Fig. 3. Schematic diagram of the Fe-redox cycle. Light-stippled areas represent solid phases, black arrows are solid-phase fluxes. White-outlined black arrows indicate reactions, white arrows are diffusion pathways. Ferric oxyhydroxides precipitated in the water column and at the sediment/water interface scavenge PO_4 and some F from seawater. During burial and mixing, microbial decomposition of organic matter utilises a sequence of electron acceptors in order of decreasing thermodynamic advantage. Oxygen is used first, followed by nitrate (and nitrite), manganese- and iron-oxyhydroxides and sulphate, in that order (Froelich et al. 1979). Degradation of organic matter liberates PO_4^{3-} to solution, and dissolution of FeOOH liberates Fe^{2+}, PO_4^{3-} and F^-, causing elevated concentrations of these ions (e.g. Fig. 2) in porewaters. If sufficient levels are attained, PO_4^{3-} reacts with Ca^{2+}, Mg^{2+} SO_4^{2-} and F^- ions diffusing into the sediment from seawater, and CO_3^{2-} derived from the oxidation of organic matter, to precipitate a precursor phosphate which subsequently recrystallises to francolite (see text for discussion). Excess PO_4^{3-} diffuses upwards towards the sediment/water interface where it is resorbed by ferric oxyhydroxides. Iron diffuses both downwards to be fixed as FeS under anoxic conditions, and upwards to the oxic layer where it is reprecipitated as FeOOH. The Fe-redox cycle, therefore provides an effective means of trapping PO_4^{3-} in the sediment and promotes the precipitation of francolite.

Iron-redox cycling of phosphorus probably occurs more generally in marine shelf sediments (Ruttenberg & Berner 1993), but does not normally lead to the precipitation of significant amounts of francolite. However, the permanent burial of iron-bound phosphorus probably takes place in a wide range of sedimentary environments, and may represent a major, and underestimated, phosphorus flux from the oceans (Berner et al. 1993; Krajewski et al. 1994). In the case of the East Australian Shelf, it is noteworthy that although sulphate reduction has been detected in anoxic microniches, francolite precipitation is essentially a suboxic (i.e. non-suphidic) process. Similarly, since glauconites contains both Fe^{2+} and Fe^{3+} (the latter predominating), precipitation of that mineral probably also occurs close to the oxic/suboxic interface.

The coupled cycling of Fe with F and PO_4^{3-} across the oxic/suboxic redox boundary (Fig. 3) means that off East Australia, apatite precipitation occurs almost entirely in the uppermost 20 cm of the sediment column, and only proceeds while nodules remain in the mixed layer, continuing for periods of more than 60 kyr. This process can produce phosphorite nodules containing up to 10% Fe_2O_3. Seafloor weathering of glauconites and other iron-bearing phases plus goethite precipitation cause further enrichment, with some seafloor conglomeratic deposits attaining 50% Fe_2O_3. However, such nodules display Na- and SO_3-depleted 'altered' francolite compositions.

It appears likely that Fe-redox cycling plays a major role in francolite precipitation in many organic-poor environments. The importance of such cycling is less clear in organic-rich deposits such as those on the Peru margin where Fe_2O_3 contents are typically less than 0.5% (Glenn & Arthur 1988), and in ancient Fe-poor phosphorites such as the Upper Cretaceous phosphatic chalks of NW Europe (Jarvis 1992). Iron-redox cycling undoubtedly provides one method of concentrating PO_4^{3-} in porewaters. Whether absorption by ferric oxyhydroxides always provides the primary means of extracting PO_4^{3-} from seawater seems unlikely, given that high levels of: (a) phosphatic fish debris; (b) planktonic organic matter; (c) benthonic microbial organic matter, have been identified in many areas (see Krajewski et al. 1994 for further discussion), and all of these are capable of yielding high levels of PO_4^{3-} to the sediment.

Trace elements

The 'open' apatite structure facilitates numerous trace-element substitutions (Tab. 1), and many elements are known to be enriched in phosphorites relative to "average" shale (Tab. 3). It is widely recognised (Gulbrandsen 1966; Tooms et al. 1969; Nathan et al. 1979; Altschuler 1980; Prévôt 1990) that an enriched trace-element group comprising Ag, Cd, Mo, Se, U, Y, Zn and the rare-earth elements (REEs: La, Ce, Pr, Nd, Sm, Eu, Gd, Tb, Dy, Ho, Er, Tm, Yb, Lu) characterise the phosphorite facies. Several other elements including Br, Cu, Cr, I, Pb & V (Prévôt & Lucas 1979, 1980, 1985; Pacey 1985; Piper 1991; Jarvis 1992) also commonly show strong affiliation to the apatite fraction in sediments. Recently, mineral structural studies using electron-spin resonance (ESR) have confirmed that many trace elements may replace Ca^{2+} in the apatite structure, including Pb^{3+} (Gilinskaya 1993), VO^{2+} (Gilinskaya & Zanin 1983), U^{4+} and Th^{4+} (Gilinskaya 1991, 1993; Gilinskaya et al. 1993). However, two points have to be made:

Tab. 3. Concentration of trace elements (μg g^{-1}) in marine phosphorites relative to "average" shale

Element	Average shale	Enrichment factor	Normal abundance	Depletion factor
Ag	0.07	30		
As	13		N	
B	100			6
Ba	580		N	
Be	3		N	
Cd	0.3	60		
Co	19			3
Cr	90		N	
Cu	45		N	
Ga	19			5
Hg	0.4			7
La	40	4		
Li	66			13
Mo	2.6	4		
Ni	68		N	
Pb	20	2		
Sc	13		N	
Se	0.6	8		
Sn	6			2
Sr	300	2		
U	3.7	30		
V	130		N	
Y	26	10		
Yb	2.6	5		
Zn	95	2		
Zr	160			2

After Altschuler (1980, Tab. 5); average shale values from Turekian & Wedepohl (1961);
N = 'normal' abundance, within a factor of 2 of the concentration in shale

(1) trace elements are not necessarily located within the apatite structure; they may be adsorbed onto crystal surfaces or may be related to another mineral or phase, particularly organic matter and sulphides;
(2) average values may be misleading, since very wide ranges of concentration exist in different deposits.

The study of trace elements is of commercial interest because of their importance as saleable by-products (U; REEs) or because of their toxicity (Cd; U-derived radionuclides), and their consequent detrimental influence on the environment either in fertilisers or in phosphogypsum. The following discussion will concentrate on members of these groups.

Cadmium and Zinc

Cadmium and Zn constitute a pair of trace elements which are closely associated in most rock types. Cadmium is the trace-element which above all others is most enriched in phosphorites compared with other lithologies (Altschuler 1980; Slansky 1980, 1986; Baturin & Oreshkin 1984), with concentrations in the order of 20 $\mu g\ g^{-1}$ being common, compared with 0.3 $\mu g\ g^{-1}$ in "average" shale. Some deposits have even higher Cd contents. Upper Cretaceous-Palaeogene phosphorites from Senegal, Togo and parts of the Gafsa Basin of Tunisia (Menor 1975; Baechle & Wolstein 1984; Johnson 1987) contain averages of 53–84 $\mu g\ g^{-1}$ Cd, while the Middle Miocene phosphorites of the US Monterey Formation (Altschuler 1980) yield 200 $\mu g\ g^{-1}$ Cd!

Cadmium correlates strongly with Zn in many phosphorites, although the former element shows considerably less enrichment in comparison to other sedimentary rocks (Tab. 3), typically occurring at around 200 $\mu g\ g^{-1}$ (compared to 95 $\mu g\ g^{-1}$ for "average" shale). The Cd-Zn relationship is in some, but certainly not all, cases attributable to the presence of sphalerite (Altschuler 1980; Minster & Flexer 1991). Generally, the two elements do not correlate with either the francolite or organic-matter fractions (Prévôt 1990; Nathan et al. 1991; Piper 1991). Altschuler (1980) and Middelburg & Comans (1991), amongst others, have argued that Cd enrichment in phosphorites is due in large part to its substitution for Ca^{2+} in the apatite structure; in contrast, the much smaller ionic radius of Zn^{2+} makes incorporation of this element less favoured. However, it should be noted that Cd has a tendency to form covalent bonds, so it does not easily replace Ca in francolite.

Cadmium and Zn, and to a lesser extent many other trace-elements including Cu and Ni, display nutrient-like [PO_4^{3-}, NO_3^-, $Si(OH)_4$] distribution in the oceans. All of these elements are highly depleted in surface waters because of their preferential extraction by marine phytoplankton during photosynthesis (Martin & Knauer 1973; Boyle et al. 1976; Boyle 1981; Bruland 1983; Price & Morel 1990; Piper 1994), but are enriched at depth as bacterial degradation of organic matter in the water column returns them to solution. It has been shown that Cd may substitute for Zn in some metalloenzymes and can promote the growth of phytoplankton in Zn-limited environments. Cadmium shows the closest correspondence to PO_4 profiles amongst all of the trace elements, and this has led to the suggestion that the Cd content of foraminiferal calcite may be used as a palaeoproductivity indicator.

The above observations, together with evidence that Cd may be concentrated further by marine bacteria (Gauthier et al. 1986), make a biogenic source of Cd in phosphorites very likely. Elemental ratios for the marine fractions of Cd, Cu, Ni and Zn in the Tertiary phosphatic sediments of both the US Monterey Formation, California (Piper & Isaacs 1994), and the San Gregorio Formation of Baja California, Mexico (Piper 1991), approach plankton values. Interestingly, the accumulation rates for these minor elements require a high rate of primary productivity, comparable to the modern Peru Shelf, which is compatible with the operation of an active upwelling regime during phosphogenesis. Interelement relationships and calculated accumulation rates for Cd, Cu, Zn, and possibly Ni, in the US Permian Phosphoria Formation of Idaho (Piper & Medrano 1994) are also consistent with a biological origin. Nonetheless, despite strong evidence for a marine plankton source of trace elements in these and other phosphorites, there remains consid-

erable uncertainty regarding their mineralogical affinities and the incorporation mechanisms involved.

Rare-earth elements and yttrium

For more than a century (Cossa 1878), the REEs have been recognised as generally being enriched in phosphate deposits (McKelvey 1950; Altschuler et al. 1967) compared to other sedimentary rock types. "Average" phosphorite (Altschuler 1980) contains 462 $\mu g\ g^{-1}$ REEs plus 275 $\mu g\ g^{-1}$ Y, while "average" shale contains only 220 and 30 $\mu g\ g^{-1}$ respectively. The bulk of the REEs and Y apparently reside in francolite, with the substitution of REE^{3+} and Y^{3+} for Ca^{2+} (Tab. 1) in one or both of the 7- and 9-fold co-ordination sites. Generally, granular phosphorites exhibit higher REE/P ratios than their nodular equivalents (Ilyin & Ratnikova 1976; McArthur & Walsh 1984; Jarvis 1984, 1992; Piper et al. 1988). Moreover, a range of distribution patterns is known, and differences in concentration of more than two order of magnitudes have been reported.

Traditionally, phosphorites have been considered to be characterised by a so-called "seawater" pattern (Goldberg et al. 1963; Altschuler et al. 1967), which is strongly depleted in Ce and enriched in the heavy REEs (HREEs; Ho-Lu) when compared with shales. This pattern, and particularly Ce depletion, is a feature of many oceanic sediments, and for comparative purposes is commonly expressed as an anomaly, calculated (Elderfield & Greaves 1982) as:

$$Ce^* = \log\ [3Ce_{sn}/(2La_{sn}+Nd_{sn})] \qquad (1)$$

where "sn" represents a concentration normalised to shale.

The typical seawater-like pattern of phosphorites (Fig. 4) would suggest that REEs in francolites were incorporated from seawater with no significant fractionation. Many important deposits, including the western US Permian Phosphoria Formation, Upper Cretaceous and Palaeogene Abu Tartur and Nile Valley deposits of Egypt, Gafsa-Metlaoui Basin of Tunisia, and Ganntour Basin of Morocco, and the late Tertiary Bone Valley Formation of Florida, (Altschuler et al. 1967; El-Kammar et al. 1979; McArthur & Walsh 1984; Tlig et al. 1987), do indeed have markedly negative Ce-anomalies, although not all display HREE enrichment.

Much current phosphorite research is dealing with REE distributions and their significance. Jordanian (Ruseifa and Eshidiya deposits; Jallad et al. 1989, Abu Murry 1993) and French (Picardy phosphatic chalks; Jarvis 1984, 1992) Upper Cretaceous phosphorites (Fig. 4), for example, are enriched by a factor of two in REEs relative to 'average' shale, and have typical seawater-like distributions, with average Ce-anomalies of –0.5 to –0.6 and enrichment in HREEs. Eocene-Miocene deep-water seamount phosphorites from the equatorial Pacific (Hein et al. 1993) also exhibit large negative Ce-anomalies. Phosphatic rocks from the western part of the Palaeogene Senegal Basin display seawater-like patterns, the details of which appear to correlate to palaeowater-depth (Bonnot-Courtois & Flicoteaux 1989; Flicoteaux et al. 1993). Cape de Naze samples of earliest Eocene age have the largest negative Ce-anomaly (–0.78) and represent a deep-water facies. Lam Lam – Taiba samples of Middle Eocene to Oligocene age seem to be related to transitional environments between platform and deep water, and have lower Ce-

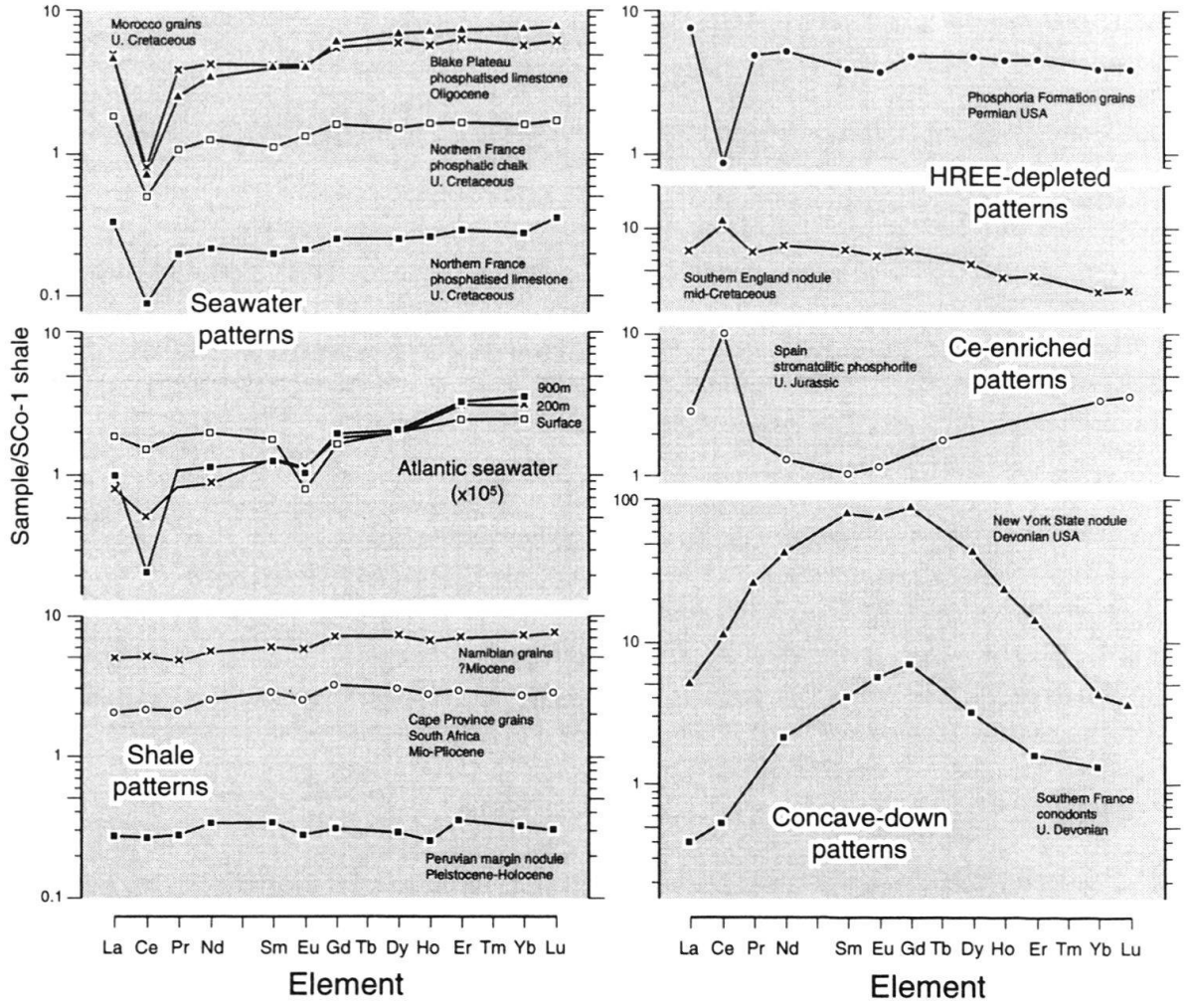

Fig. 4. Shale-normalised rare-earth element (REE) distributions for selected phosphorites. Seawater-like patterns with negative Ce-anomalies and enrichment in the heavy REEs (top left) are typical of many phosphorites, but flat shale-like patterns (bottom left) are also common (see text for discussion). Shale values (USGS shale reference material SCo-1) from Potts et al. (1993b). Seawater data from Elderfield & Greaves (1982); phosphorite data from McArthur & Walsh (1984), Jarvis (1992; N. France samples) and Martin-Algarra et al. (1993; Spanish sample); conodont data from Grandjean-Lécuyer et al. (1993).

anomalies of between –0.62 and –0.72. Similar depth-related trends have been identified (Grandjean et al. 1987) in REE data from Upper Cretaceous – Middle Eocene fish teeth from Moroccan phosphorites, and have been suggested, but not yet corroborated, for the Oligo-Miocene deposits of Baja California Sur, Mexico (Piper 1991). These trends are consistent with those shown by dissolved REEs in modern seawater. Modern coastal and ocean-surface waters generally have little or no negative Ce-anomaly and little HREE enrichment (e.g. Elderfield & Greaves 1982; Bertram & Elderfield 1993), but both features develop progressively with depth (Fig. 4) to form more typical "seawater" patterns by around 1 km in the open ocean.

With the notable exception of some phosphatised limestones, most Miocene – Holocene offshore phosphorites from Namibia, Cape Province and Agulhas Bank of South Africa (McArthur & Walsh 1984; Nathan et al. 1993), and the Peru margin (Piper et al. 1988), have shale-like REE distributions (Fig. 4) with no Ce anomaly. Phosphatic micro-

stromatolites from the Lower Cambrian in the Algerian Sahara (Bertrand-Sarfati et al. 1993) and coeval deposits at Karatau, Kazakhstan (Semenev et al. 1962) have similar patterns. Unusually, stromatolite-related Upper Jurassic phosphorites from Spain (Martin-Algarra et al. 1993) display a variety of REE distributions ranging from relatively flat shale-like patterns to those with large positive Ce-anomalies (Fig. 4) of up to +1.27. In the latter case, the REEs appear to be related to iron and manganese oxyhydroxide phases in the phosphorite.

Variations in Ce anomalies might in some cases be controlled by oxygenation levels (Elderfield & Pagett 1987; Wright et al. 1987), since fish remains from anoxic basins and shelves exhibit very small negative to moderate positive Ce-anomalies, while well-oxygenated outer shelf and deep-ocean deposits show moderate to large negative Ce-anomalies. However, local positive Ce-anomalies of +0.5 have also been identified in suboxic porewater underlying seawater with a negative anomaly (Elderfield & Sholkovitz 1987), so the degree to which Ce anomalies are controlled by seawater as opposed to porewater composition and redox-state remains open to debate.

Many biogenic phosphates, including Upper Palaeozoic conodont elements (Wright et al. 1987; Grandjean & Albarède 1989; Grandjean-Lécuyer et al. 1993), and both Triassic and Eocene fish teeth from France, show unusual REE patterns. These are strongly depleted by up to one order of magnitude in both the heavy and light REEs compared to the intermediate REEs, producing strongly concave-down patterns (Fig. 4) centred on Eu and Gd. A Devonian phosphate nodule from New York State in the US (McArthur & Walsh 1984) and Lower Carboniferous (Tournaisian; Notholt pers. comm. 1994) nodules from the Montagne Noire, France (Tlig et al. 1987), have similar patterns. Concave-down REE distributions have been reported (Hoyle et al. 1984) for μm-scale particulate and colloidal matter from modern river-seawater mixing zones, offering the possibility that the Palaeozoic phosphates acquired their REEs during diagenesis in estuarine or coastal settings. Unfortunately, this suggestion does not appear to be consistent with geological evidence, which indicates that the majority of samples originated from well-oxygenated shallow-water (<100 m) carbonate-shelf environments of normal marine salinity. Whether these patterns reflect unmodified seawater compositions remains controversial, but Nd-isotope studies (see below) support such a conclusion.

Recently, Grandjean-Lécuyer et al. (1993) have argued that prior to the evolution of modern open-ocean plankton during the early Cretaceous, the REE distribution of seawater was not controlled by ocean-surface biological productivity, but by inorganic processes associated with the scavenging of REEs by ferric oxyhydroxides. These authors argued that fractionation associated with these processes led to a characteristic concave-downwards profile in pre-Cretaceous seawater which was transferred unaltered to biogenic apatites. This suggestion seems oversimplistic. Not all pre-Cretaceous phosphorites display such patterns. Phosphoria Formation grains of Permian age, for example, have slightly HREE-enriched patterns with large negative Ce-anomalies (Fig. 4). On the other hand, Eocene fish teeth have been described (Grandjean & Albarède 1989) with strongly concave-downwards patterns. It must be concluded that although removal processes may promote different REE patterns in phosphate, such patterns are not necessarily global in distribution.

The REEs in francolite may be derived from: (1) seawater directly; (2) ferromanganese oxide-organic matter particles; (3) biogenic silica; (4) siliciclastic debris, particularly

clay minerals; (5) precursor carbonates. Simple mass-balance arguments indicate that given the relatively large size (and proportionally small surface area) of biogenic phosphate and phosphorite grains, and the very low concentrations (fg g^{-1}) (femtogram = 10^{-15} gram) of REEs in seawater, incorporation is unlikely to occur directly. It almost certainly takes place during early diagenesis, following the release of REEs from dissolving carrier phases, particularly sub-μm scale ferromanganese oxyhydroxides particles and grain-coatings and organic matter (cf. Jarvis 1984, 1992; Sholkovitz et al. 1989), which have previously scavenged large quantities of REEs from the water column. Reduced sedimentation and burial rates favour increased concentrations of REEs in francolite (Jarvis 1984; Elderfield & Pagett 1986; Wright et al. 1987), since the longer the mineral remains close to the oxic/suboxic redox boundary, the longer it is able to incorporate REEs being liberated from their carriers. Concentration levels also appear to be related to grain-size and possibly to kinetic effects. In most cases, additional sources of REEs such as siliciclastic and biogenic detritus and precursor carbonate grains, matrix and cements are unlikely to provide the quantities of REEs necessary to produce the enrichment levels observed in phosphorites. Nonetheless, biogenic silica has been advocated as a source of REEs in some deposits (Piper 1991).

McArthur & Walsh (1984) suggested that francolites precipitate with very low REE contents, but subsequently scavenge REEs from other sources throughout their history, so old onshore deposits contain the highest REE contents. This hypothesis is supported by data from fish remains (teeth, vertebrae), which initially contain negligible REEs (Bernat 1975) and rapidly acquire high concentrations *post-mortem* (Grandjean et al. 1987). However, the resulting patterns appear to mimic those of the overlying water column (Wright et al. 1987), and do not appear to be modified significantly by interaction with formation or groundwaters during burial (Grandjean & Albarède 1989).

Finally, it has been shown (Bonnot-Courtois & Flicoteaux 1989; Dar'in & Zanin 1990; Flicoteaux et al. 1990) that weathering leads to the leaching, fractionation and redistribution of REEs, and may substantially modify the primary REE signature of a deposit. For any particular phosphorite, therefore, several factors are likely to have influenced the final REE content and signature. The mechanisms of REE incorporation appear to be closely tied to the organic matter degradation and redox-driven processes which, on current evidence, are so fundamental in driving phosphogenesis. However, the probability that REE patterns reflect not only their depositional environment, but also the imprint of diagenesis and weathering, clearly must be taken into account when interpreting data.

Uranium

Uranium is another of the elements generally showing strong enrichment in phosphorites (120 μg g^{-1} in "average" phosphorite, compared with 3.7 μg g^{-1} in "average" shale; Altschuler 1980). Indeed, the enrichment of phosphorites in U is so strong, that mapping the radioactivity of the seafloor using a deep-tow scintillometer (Jones 1989) is an effective way of determining the distribution of phosphatic sediments in many parts of the oceans.

Much research on U in phosphorites (McKelvey 1956; Altschuler et al. 1958) has been driven by the wish to find alternative U sources for military and civilian nuclear programmes. However, more recently, U has also been studied because of its applications in dating (Kolodny & Kaplan 1970a; Baturin et al. 1972; Veeh et al. 1973, 1974; Bur-

nett et al. 1982, 1988; Kim & Burnett 1986; Barole et al. 1987; McArthur et al. 1988), as an indicator of diagenesis (Starinsky et al. 1982), and as a potential palaeo-redox marker (Burnett & Gomberg 1977). Although there is generally a strong positive correlation between U and P contents for individual deposits (e.g. Jeanmaire 1985), it is unclear whether U is incorporated into the francolite lattice, adsorbed onto crystallite surfaces and/or associated with enclosed accessory phases, particularly organic matter. Fission-track mapping (Burnett & Veeh 1977; Kress & Veeh 1980; Avital et al. 1983) convincingly demonstrates that U is intimately associated with francolite on a microscopic scale, and ESR studies (Gilinskaya 1991, 1993; Gilinskaya et al. 1993) confirm that both U^{4+} and Th^{4+} substitute for Ca^{2+} in the structures of many natural apatites. However, in some deposits (Lucas & Abbas 1989) U is dominantly complexed by organic matter and may not be present in the apatite lattice in significant quantities.

Uranium occurs as both U(IV) and U(VI) in varying proportions in different phosphorites (Altschuler et al. 1958; Kolodny & Kaplan 1970a; Veeh et al. 1973). East Australian ferruginous phosphorite nodules (O'Brien et al. 1987), for example, range from 11–86% U(IV) and, in general, it appears that samples with high U/P_2O_5 ratios tend to contain higher proportions of U(IV). Crystallographic arguments indicate that U(IV) would be most easily accommodated by the apatite lattice, and indeed there is some evidence that U is incorporated into francolite almost entirely in that form (Altschuler et al. 1958; O'Brien et al. 1987), and is only subsequently converted to U (VI) by oxidation processes. It has also been suggested that phosphorites form initially with high U/P_2O_5 ratios, and that precipitation of later francolite in nodules is accompanied by little further U-uptake. Possible causes for this differential uptake of U include: (1) kinetic effects causing rapidly growing francolites to be depleted in U; (2) the diffusional supply of U being reduced as porosity declined during lithification; (3) a varying supply of U(IV), possibly due to differing redox conditions and availability of labile organic matter during initial and later precipitation of francolite. Uranium occurs in seawater around 3 ng g^{-1}, but is fixed and concentrated by organic complexes. Oxidation of organic matter leads to remobilisation of U as soluble U(VI) species (Colley & Thomson 1985), which may diffuse to be reprecipitated as U(IV) at the suboxic/oxic redox interface. Consequently, it is likely that redox-cycling also plays an important role in controlling the U supply to phosphorites.

Uranium contents vary enormously between different deposits (Cathcart 1978, 1992; Slansky 1980, 1986). For example, despite typical phosphorite concentrations of >100 μg g^{-1} U, many Cambrian examples in Siberia contain only 4 μg g^{-1} (Ilyin pers. comm. 1993), and relatively low U concentrations (5–12 μg g^{-1}) appear to be common in many other Proterozoic-Cambrian phosphorites (e.g. Mongolia, 2–11 μg g^{-1} U in the Khubsugul phosphorites, Ilyin et al. 1986; Upper Volta, 4–8 μg g^{-1} U in the Tapoa deposits, Lucas et al. 1986; Kazakhstan, 4–8 μg g^{-1} U in Karatau phosphorites, Ilyin pers. comm. 1993). Low U concentrations of this order are also typical of Tertiary seamount phosphorites (Kolodny 1981; Roe & Burnett 1985; Cullen & Burnett 1986; Hein et al. 1993). At the other extreme, Eocene deposits near Bakouma (Central African Republic) contain 1660–5600 μg g^{-1} U (Gony 1971), and some Middle Palaeozoic phosphorites in Siberia yield up to 4000 μg g^{-1} U (Gavshin et al. 1974). Such extreme variation is almost certainly a consequence of post-depositional diagenetic, hydrothermal, metamorphic and/or weathering effects, all of which may cause significant U mobilisation (Altschuler et al. 1958; Cook 1972; Cathcart 1978; Slansky 1980, 1986; Jeanmaire 1985; McArthur & Herczeg 1990).

Much remains to be understood about the locations and mechanism of incorporation of U in phosphorites. It is now clear, however, that high U concentrations and high proportions of U(IV) in phosphorites do not necessarily indicate that francolite precipitation occurred under anoxic conditions, nor do they equate directly with deposition in organic-rich sediments. Indeed, nodules precipitated in association with organic-rich muds on the Peru margin commonly contain less U and more U(VI) than those accumulating in glauconitic foraminiferal sands off East Australia.

Isotope geochemistry

The chemistry and relative stability of francolite makes it perhaps *the* most versatile sedimentary mineral for isotope studies. Many of the stable and radiogenic isotopes which are used as tracers or dating devices in sedimentary rocks occur in francolite (Fig. 5, Tab. 4). The three most commonly used elements for stable-isotopic work, O, C and S, are all major structural components of francolite, while three major radiogenic isotope tracers Sr, Nd and U, are constituents that replace major elements in the lattice.

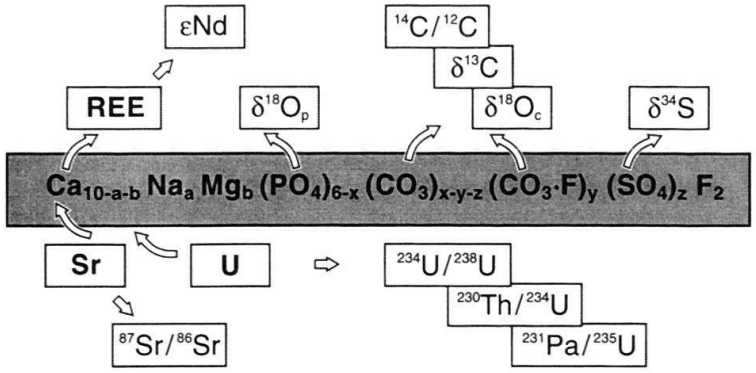

Fig. 5. Schematic diagram showing the location of different isotopes in francolite. Note the stable and radiogenic isotopes of the light elements are constituents of major anions in francolite, whereas the radiogenic isotopes of the heavy elements are trace substituents for the Ca cation.

Oxygen stable-isotopes

The use of oxygen-isotope ratios in marine carbonate CO_3^{2-} to estimate water palaeotemperatures (Urey et al. 1951) and to determine diagenetic conditions (Hudson 1977; Irwin et al. 1977) is well-established. For most purposes the $^{18}O/^{16}O$ ratio is expressed in delta (δ) notation as a per mille (‰) deviation from an ocean water (SMOW – Standard Mean Ocean Water) or calcite (PDB – Pee Dee Belemnite) standard. Francolite offers the rare opportunity of determining the oxygen-isotope ratios of two cogenetic pairs in a single mineral, $\delta^{18}O_p$ of PO_4^{3-} and $\delta^{18}O_c$ of CO_3^{2-}.

The application of variations in the $\delta^{18}O_p$ of phosphatic fish debris as an indicator of modern and ancient water temperatures has been demonstrated (Longinelli & Nuti 1973a, b; Kolodny et al. 1983; Kolodny & Raab 1988; Kolodny & Luz 1992b). The proposed phosphate-water temperature equation (Longinelli & Nuti 1973a) is:

$$T\,^{\circ}C = 111.4–4.3\,(\delta^{18}O_p–\delta^{18}O_w) \qquad (2)$$

where T is the average environmental temperature, $\delta^{18}O_p$ is francolite phosphate and $\delta^{18}O_w$ is that of the water, both on the SMOW scale. Revised empirical equations have been published by Karhu & Epstein (1986), Shemesh et al. (1988) and Kastner et al. (1990).

Tab. 4. Isotopes in francolite and their applications

Element	Parameter measured	Genesis of phosphorites	About the World
Ca-sites			
Sr	$^{87}Sr/^{86}Sr$	age	land – sea distribution
Nd	εNd		land – sea distribution palaeoceanography
U	$^{234}U/^{238}U$ $^{230}Th/^{234}U$ $^{231}Pa/^{235}U$	rate of growth, age	
PO_4-site			
O	$\delta^{18}O_p$, $\delta^{18}O_c$	temperature of formation, diagenetic environment	palaeoclimate
C	^{14}C	age	
	$\delta^{13}C$	diagenetic environment	
S	$\delta^{34}S$	diagenetic environment	

Modified from Kolodny & Luz (1992)

The $\delta^{18}O_c$ equation for apatite is assumed to be the same as $CaCO_3$ (Epstein et al. 1953):

$$T\,°C = 16.5–4.3\,(\delta^{18}O_c–\delta^{18}O_w) + 0.14\,(\delta^{18}O_c–\delta^{18}O_w)^2 \quad (3)$$

where $\delta^{18}O_c$ is francolite carbonate.

In both cases, the $\delta^{18}O$ of the water has be known or estimated to obtain a unique palaeotemperature. Most offshore Tertiary and Quaternary phosphorites yield $\delta^{18}O_c$ values (Kolodny & Kaplan 1970b; McArthur et al. 1980, 1986) which are consistent with precipitation in equilibrium with marine waters at palaeoceanographically reasonable water temperatures (typically 6–20 °C). Namibian concretions, for example, yield $\delta^{18}O_c$ temperatures of 6–13 °C, which are within the range of temperatures (6–16 °C) measured for modern upwelling water on the margin. However, many onshore deposits (e.g. Jordanian Upper Cretaceous Al-Hasa deposit, US Permian Phosphoria Formation, Australian Middle Cambrian Georgina Basin phosphorites) exhibit anomalously light compositions which have been attributed to weathering effects caused by interaction with isotopically light (i.e. ^{16}O-enriched) groundwaters (Shemesh et al. 1983; McArthur et al. 1986). By contrast, Piper & Kolodny (1987) argued that $\delta^{18}O_p$ values from their Phosphoria Formation samples are unaltered and indicate high Permian palaeowater temperatures of 33.7–40.4 °C. Stratigraphic variation was interpreted as reflecting glacial-interglacial cyclicity and the consequent change in the $\delta^{18}O$ composition of seawater. High Oligo-Miocene palaeowater temperatures of 27.5–32.7 °C were also suggested by Piper (1991) based on $\delta^{18}O_p$ data from deposits of Baja California Sur, Mexico.

It is generally agreed that although $\delta^{18}O_c$ is more susceptible to alteration than $\delta^{18}O_p$ (Shemesh et al., 1983, 1988; McArthur & Herczeg 1990), isotopic exchange may occur

from both sites, and $\delta^{18}O_p$ does not provide the perfect palaeothermometer it was once held to be. When phosphorites of different ages are compared (Longinelli & Nuti 1968; Shemesh et al. 1983, 1988; Karhu & Epstein 1986), $\delta^{18}O_c$ and $\delta^{18}O_p$ display clear, roughly parallel, exponential trends of decreasing values with age, the greatest changes occurring during the last 100 Myr. This major shift must be due in part to falling global temperatures since the Late Cretaceous, but pre-Cretaceous values are almost certainly altered. Carbon isotopes show no such relationship.

In some ancient phosphorites coexisting fish material and francolite cements have comparable $\delta^{18}O_p$ values, which yield geologically reasonable palaeotemperatures. Shemesh & Kolodny (1988), for example, interpreted stratigraphic variation of $\delta^{18}O_p$ in Upper Cretaceous Mishash Formation phosphorites and fish remains, as indicating that a cool-water upwelling episode was associated with a major phosphogenic event in SE Tethys. In other deposits, such as the Middle Miocene Monterey Formation of California (Kastner et al. 1990), $\delta^{18}O_p$ values of fish debris are considerably higher (by up to 6‰) and much less variable than associated phosphorites, suggesting that significant post-depositional isotopic exchange has occurred in the latter. Only fish-derived data consistently indicate viable palaeowater temperatures of 11–25 °C.

Variation in the isotopic composition of O in response to temperature for the carbonate and phosphate sites in francolite, is sufficiently different to offer the possibility of determining palaeotemperatures from $\delta^{18}O_c - \delta^{18}O_p$ pairs, independently of water compositions. Unfortunately, although trends for the two ratios are collinear, late diagenetic interaction with formation (Shemesh et al. 1988; Kastner et al. 1990) or meteoric (McArthur & Herczeg 1990) waters commonly lead to diagenetic rather than depositional palaeotemperatures being recorded. Particularly in organic-rich sediments, reequilibration may occur even at relatively low water/rock ratios, and it remains unproved that precipitation invariably occurs under equilibrium conditions. Consequently, the interpretation of phosphorite oxygen-isotope data remains highly problematic.

It must be concluded that the use of $\delta^{18}O$ data to estimate seawater temperatures or isotopic compositions should be undertaken with the greatest caution. Available evidence indicates that biogenic apatites are less prone to late diagenetic overprint than coexisting grain and nodule francolite cements, although even the former are liable to be affected under some circumstances. Nonetheless, deposits which have never been buried deeply and have experienced little movement of formation waters may still retain a depositional signature.

Carbon stable-isotopes

In addition to measuring $\delta^{18}O$ in francolite CO_3^{2-}, it is also possible to determine the $^{13}C/^{12}C$ ratio ($\delta^{13}C$, reported as a ‰ deviation from the PDB standard). Used together, $\delta^{18}O_c$ and $\delta^{13}C$ data (Fig. 6) are highly instructive concerning the physicochemical conditions of francolite precipitation. It is necessary to make several assumptions concerning the timing and mechanism of incorporation of CO_2 in the apatite lattice:

(1) little or no carbon-isotope fractionation occurs during incorporation of carbonate, so values are representative of dissolved CO2 in the water from which the mineral precipitated;

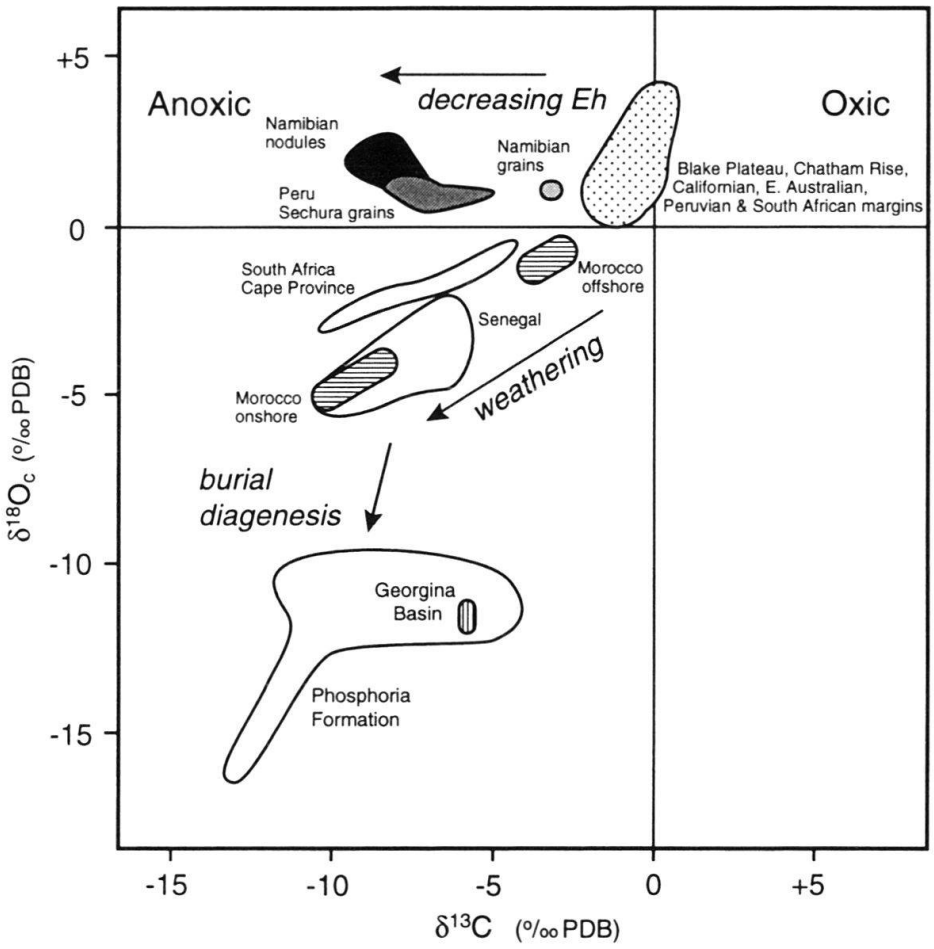

Fig. 6. Variation of $\delta^{13}C$ and $\delta^{18}O$ in modern and ancient francolite carbonate (based on McArthur et al. 1986 with Senegal data from Girard et al. 1993).

(2) carbonate enters the lattice at the time of precipitation;
(3) isotopic re-equilibration has not occurred subsequently.

By analogy to $CaCO_3$ precipitation, carbon isotope fractionation is expected to be minimal. This assumption is supported by a preponderance of seawater-like $\delta^{13}C$ values reported for francolites from Tertiary and Quaternary seafloor phosphorites (Kolodny & Kaplan 1970b; McArthur et al. 1980, 1986; Benmore et al. 1983, 1984; Shemesh et al. 1988). However, the range of CO_2 contents exhibited by individual phosphorites suggests that precipitation is not instantaneous and occurs within a 'window' of evolving pore-water compositions. Furthermore, in the case of biogenic phosphates, CO_2 is added *post mortem* during the transition of the original hydroxyapatite to francolite, which must take place by a dissolution-reprecipitation process.

The use of $\delta^{13}C$ data to constrain depositional and early diagenetic environments hinges on our understanding of the isotopic fractionation which occurs during the microbial degradation of organic matter in sediments (Irwin et al. 1977; Froelich et al. 1979). Marine organic matter is highly depleted in ^{13}C, typically around –24‰ $\delta^{13}C$ PDB, and when oxidised it produces dissolved inorganic carbon (DIC) species (CO_2, HCO_3^-) of the

same isotopic composition. The amount of bicarbonate in porewaters is small, so carbon stable-isotopes in DIC are very sensitive to organic degradation processes which affect the sediment during burial (in contrast, oxygen isotope compositions are dominated by the water).

The proportion of organically-derived CO_2 (Fig. 7) varies with depth as organic matter is oxidised by a succession of bacterial populations. In the oxic and suboxic upper layers of sediment, where oxygen and then nitrate, iron and manganese compounds are used sequentially as oxygen sources, there is generally a modest increase in DIC with depth, causing decreasing porewater $\delta^{13}C$ values to a minimum of around –6‰ (or –3‰ if calcite dissolution accompanies CO_2 production). Below this, under anoxic conditions,

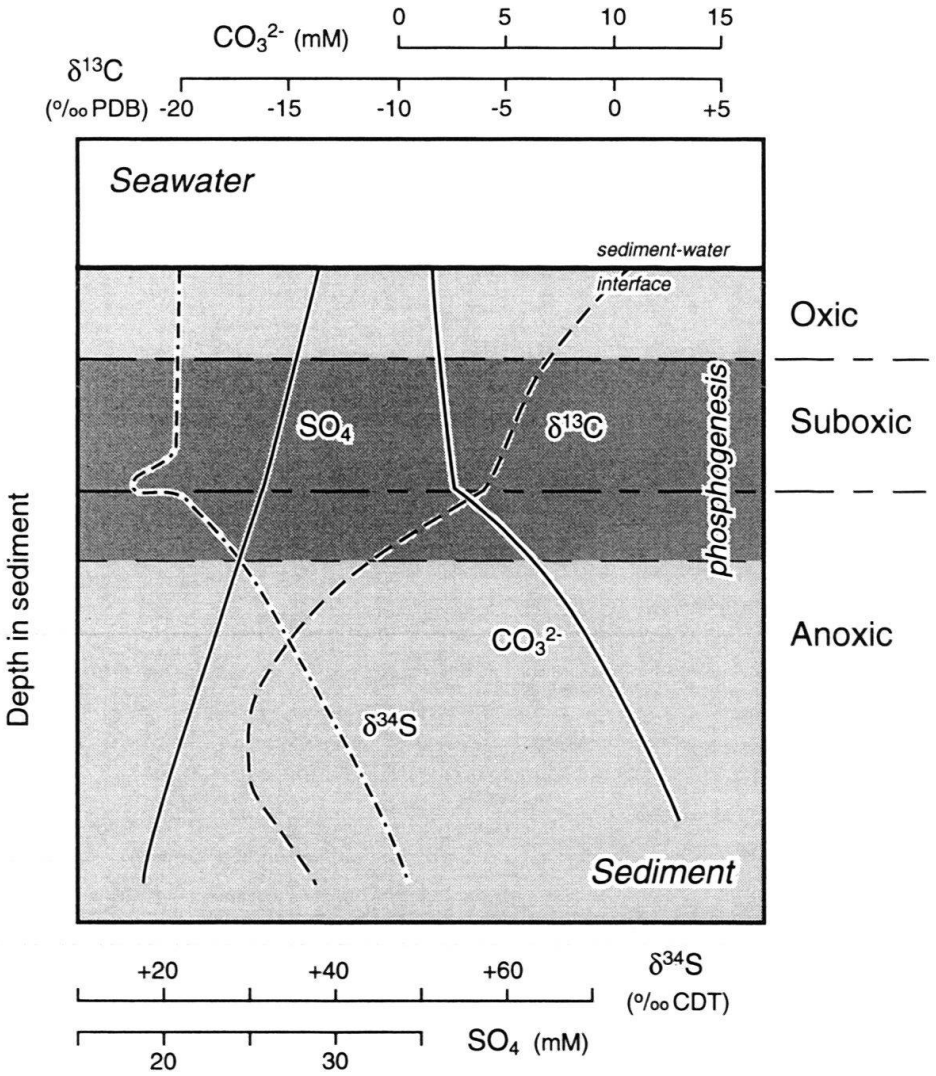

Fig. 7. Schematic diagram showing the relationships between porewater CO_3^{2-}, $\delta^{13}C$, SO_4 and $\delta^{34}S$ with increasing depth in the sediment. The CO_3^{2-} curve assumes that pH is constant and dissolved inorganic carbon (DIC) increases linearly with depth. Porewater data from modern sediments (Fig. 1, 2) and stable isotope data from modern and ancient phosphorites, indicate that phosphogenesis is confined largely to the suboxic and uppermost part of the anoxic zones (heavily stippled area). The depth and thickness of each zone varies considerably between sites in response to differences in sedimentation rate, organic carbon flux, bioturbation rate, seawater oxygen content and other factors; all three zones may not be distinguishable at all sites (modified from McArthur et al. 1986).

sulphate reduction leads to increased bicarbonate production and a pronounced decrease in $\delta^{13}C$, down to –18‰ (Fig. 2, 7).

When sulphate is exhausted, organic matter is decomposed by methanogenic microorganisms. Acetate fermentation produces isotopically very light CH_4 (< –60‰ $\delta^{13}C$) and, at least in the initial stages, CO_2 (–20‰, rising to –5‰ as the reaction progresses). At the same time, part of the total dissolved CO_2 will undergo carbon dioxide reduction by reaction with bacterially-derived hydrogen, producing additional methane which is also isotopically light (CH_4 is 25–60‰ lighter than its precursor CO_2). Consequently, cements precipitated in association with the oxidation of CH_4 have very light carbon stable-isotope signatures. However, the reservoir effect associated with carbon dioxide reduction causes the residual CO_2 to become progressively heavier, ultimately attaining values as high as + 15‰ $\delta^{13}C$. In practice, such extremes are quite rare (Emery & Robinson 1993), and cements precipitated in the methanogenic zone are typically between + 2 and – 22‰.

The carbon stable-isotope composition of francolites in replaced limestones will be influenced by the marine $\delta^{13}C$ values of their carbonate precursor, since porewater bicarbonate will generally be dominated by that source. Even in this situation, however, modification of the isotopic signature should occur. The replacement of $CaCO_3$ requires its dissolution, which is most likely a result of CO_2 production caused by the breakdown of organic matter in the oxic zone. In this situation, the reaction should buffer the $\delta^{13}C$ to a point half way between the $\delta^{13}C$ of the CO_2 and the $CaCO_3$, and the francolite precipitated should display a negative isotope signature that is the mean of the two. The signature can only remain relatively unmodified in systems with low water/rock ratios and low organic matter contents, where carbonate dissolution and francolite precipitation are not directly coupled. In organic-rich water-dominated systems even phosphatised limestones should acquire negative $\delta^{13}C$ values. Finally, although carbon isotope ratios are much less prone to alteration during deep burial and weathering than oxygen isotopes, the loss of structural-CO_2 from weathered francolites must be cause from concern. Certainly, interaction between groundwaters charged with soil-derived DIC and francolite during lateritic weathering consistently leads to light carbon (–15 to –10‰ $\delta^{13}C$) and oxygen (+22 to +27‰ SMOW $\delta^{18}O_c$) isotope values in secondary apatites (Girard et al. 1993).

Current isotopic evidence indicates that most phosphorites formed under dominantly oxic to suboxic conditions. For example, the negative correlation between francolite $\delta^{13}C$ and CO_2 values in Peru margin Holocene phosphorites (Fig. 8), with maximum CO_2 contents of 6% corresponding to minimum $\delta^{13}C$ values of around –3‰ (Glenn et al. 1988; Glenn 1990a), are consistent with precipitation within 10–20 cm of the sediment/water interface in dominantly suboxic conditions. Most other young (late Tertiary – Quaternary) seafloor phosphorites, including those from the eastern US Blake Plateau, Chatham Rise of New Zealand, East Australian margin, and off South Africa, also display $\delta^{13}C$ signatures within a few per mille of seawater values (Fig. 6). Isotopically lighter compositions (down to –15‰) characteristic of anoxic diagenesis have been recorded only from late Pleistocene – Holocene nodules off Namibia, for Tertiary phosphorites from the Ica Plateau and Sechura Desert of Peru, the Miocene of Baja California Sur (Piper 1991), and southern Florida (Compton et al. 1993), and some onshore Upper Cretaceous – Palaeogene Moroccan samples. One other notable exception has been reported (McArthur et al. 1980; Benmore et al. 1984) from the Namibian shelf, which has yielded a F-poor hydrated calcium magnesium phosphate-cemented nodule (?coprolite) containing

29.5% P_2O_5 and a phosphate-$\delta^{13}C$ value of +15.6‰. Such a heavy isotopic signature suggests that this is a rare example of phosphate precipitation during CO_2 reduction in a methanogenic environment. The unusual mineralogy of this nodule corresponds to a possible francolite-precursor (see above), yet its isotopic signature would indicate a highly evolved diagenetic history.

When plotted on a $\delta^{13}C$ versus $\delta^{18}O_c$ diagram, most ancient phosphorites fall on a broad array constrained at one end by seawater and at the other by secondary apatite (isotopically light with respect to both oxygen and carbon) compositions (Fig. 6), indicating that the former display varying amounts of alteration. Nonetheless, the broad range of $\delta^{13}C$ values for young phosphorites (+0.2 to –9‰) is similar to that of ancient phosphorites and no clear time-related trends are evident (Shemesh et al. 1988). This suggests that under favourable circumstances $\delta^{13}C$ values may be relatively well-preserved over geologic time, or if alteration occurs its end members lie within the range of original $\delta^{13}C$ values of francolites.

Studies are not limited to $\delta^{13}C$ of the apatite CO_2, important supporting data may be obtained from the $\delta^{13}C$ of associated carbonate minerals. It is known that secular variation in marine carbonate $\delta^{13}C$ has occurred through the Phanerozoic (e.g. Tucker & Wright 1990; Veizer 1992) with long-term fluctuations of –1 to +2‰ and short-term 'excursions' of between –2 and +5‰. Smaller-scale geographical and depth-related variation may also occur. Clearly, appropriate corrections need to be applied before interpreting diagenetic conditions during francolite or carbonate precipitation. Once this is accomplished, the isotopic signatures of carbonate cements and their relationship to francolite in a paragenetic sequence can provide valuable information about the conditions of phosphogenesis.

Francolite oxygen and carbon isotope ratios may be indicators of depositional or diagenetic palaeotemperatures and/or fluid compositions, so it is essential that oxygen and carbon isotopes constitute only part of a multi-element, and ideally multi-phase, isotopic and geochemical study. In such cases, it may be possible to correct for alteration effects (e.g. McArthur et al. 1987; McArthur & Herczeg 1990) and obtain initial compositions which indicate conditions at the time of formation.

Sulphur stable-isotopes

The presence of SO_4^{2-} in the francolite lattice as an isomorphous substitution for PO_4^{3-} is now generally accepted. Sulphate levels in unaltered phosphorites are close to 2.7% (McArthur 1978a, 1980, 1985). The degree of substitution depends on the SO_4^{2-} content of the aqueous phase in equilibrium with francolite (Smirnov et al. 1962; Bliskovskiy et al. 1977; McArthur 1985). The relative lack of variation displayed by unweathered francolites must reflect precipitation under similar, largely non-sulphidic, conditions, since removal of SO_4^{2-} from porewaters during sulphate reduction (Fig. 2, 7) should be reflected by declining SO_4^{2-} contents in francolites. However, it should be noted that the high concentration of sulphate in seawater, coupled with the ability of diffusion to replace SO_4^{2-} lost by the precipitation of sulphides, mean that the system is insensitive to small amounts of reduction.

Substitution of SO_4^{2-} for PO_4^{3-} in the francolite lattice offers the possibility of using sulphur stable-isotopes ($^{34}S/^{32}S$ ratios expressed as ‰ $\delta^{34}S$ CDT – Cañon Diablo Troilite)

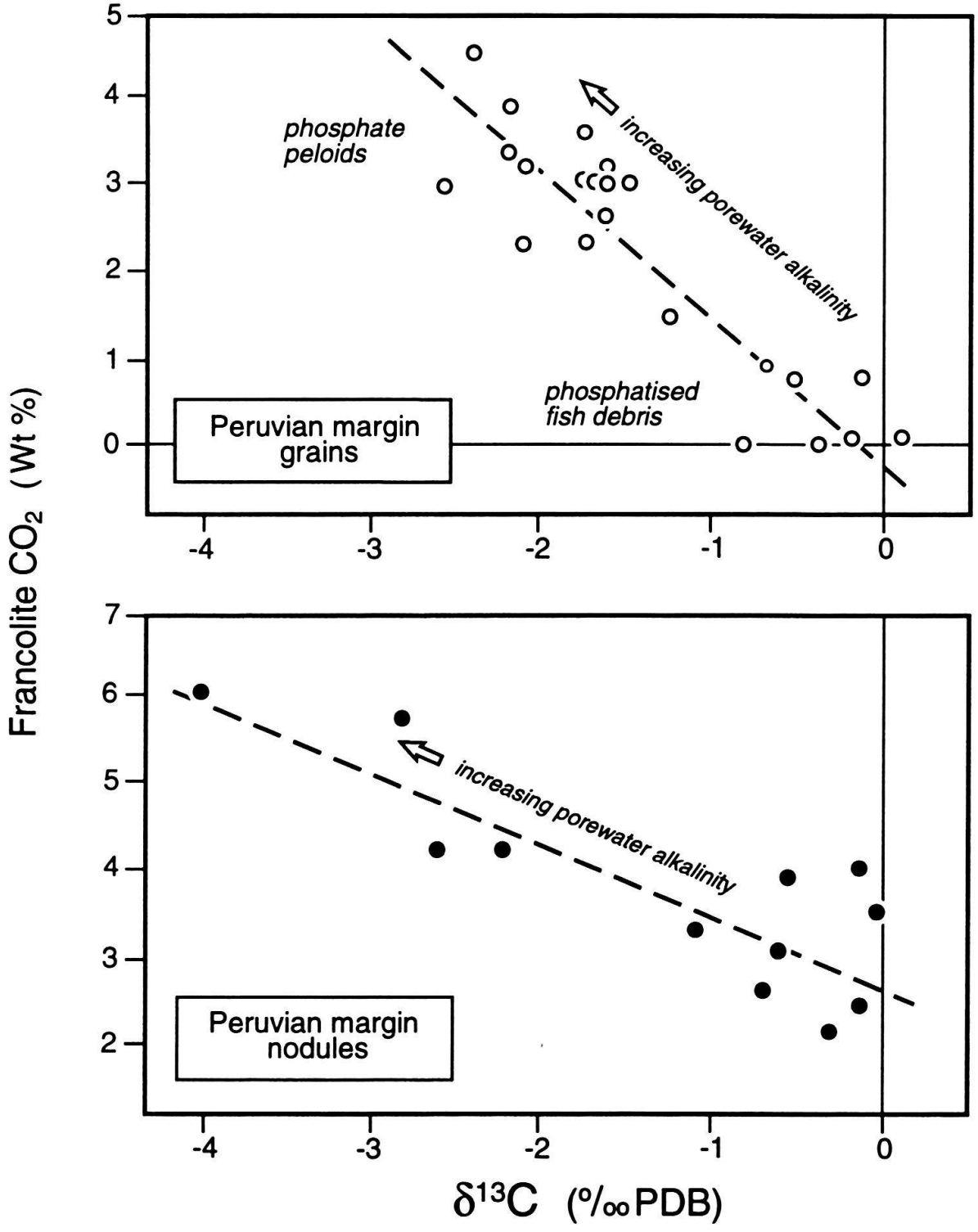

Fig. 8. Diagram showing the negative relationship between $\delta^{13}C$ and CO_2 contents displayed by francolites in modern phosphorite grains and nodules from the Peruvian margin. Grains are bulk samples; nodules are from a single locality (Station 4, 12° S); CO_2 contents calculated using the XRD method of Gulbrandsen (1970). Note the different slopes and relative positions of the two regression lines. High CO_2 and low $\delta^{13}C$ values in francolites indicate high alkalinities in associated porewaters, which ultimately limit phosphate precipitation (modified from Glenn et al. 1988, Glenn 1990a).

to constrain the origin of phosphorites (Bliskovskiy et al. 1977; Nathan & Nielsen 1980; Benmore et al. 1983; McArthur et al. 1986; Piper & Kolodny 1987; Compton et al. 1993). The residence time of SO_4^{2-} in the oceans is very long, in the order of 12 Myr, several orders of magnitude longer than oceanic mixing times of 1.5 kyr and the oceanic residence time of phosphorus (Ruttenberg 1993) of 16–38 kyr, so the isotopic composition of modern seawater sulphate is globally uniform, with values of around +23 $\delta^{34}S$. Nonetheless, on a geological timescale it has varied between +10 and +30‰ $\delta^{34}S$ (Claypool et al. 1980), in response to changing proportions of oxidised and reduced sulphur being buried as evaporites or sulphides and organic compounds, respectively.

Sulphur retains a seawater isotope composition in the oxic and suboxic zones (Fig. 7), but sulphate reduction leads to strong fractionation, commonly between 25 and 50‰, with the reduced phase being enriched in ^{32}S and residual sulphate becoming increasingly isotopically heavy. However, the degree of fractionation is inversely related to the rate of sulphate reduction (Kaplan 1983), so for sediments which are very rich in easily metabolisable organic matter the fractionation may approach zero or even reverse. In contrast, by analogy to evaporite sulphate precipitation, little fractionation (only about +1.5‰; Claypool et al. 1980) should occur during the incorporation of SO_4^{2-} by francolite. Consequently, francolite precipitating from porewaters will record the $\delta^{34}S$ sulphate values at the time of precipitation, and after correction for seawater composition ($\Delta^{34}S = \delta^{34}S_p - \delta^{34}S_w$) should differentiate between oxic and anoxic environments. Precipitation of francolite during sulphate reduction has been suggested (Nathan & Nielsen 1980; Piper & Kolodny 1987) for Phosphoria Formation phosphorites, in which a strong negative correlation between SO_4^{2-} and $\delta^{34}S$ values has been observed, supporting dominantly Rayleigh distillation-type reduction of sulphate to sulphide in a closed porewater system. It is unlikely in this case that low SO_4^{2-} values are due to weathering, because they are associated with a shift towards isotopically heavy $\delta^{34}S$, rather than the light values which are typical of alteration by meteoric waters.

From the above arguments, one would generally expect a positive correlation between isotopically light $\delta^{13}C$ and positive $\Delta^{34}S$ values in francolites. Late Tertiary – Quaternary seafloor phosphorites from the Blake Plateau, Chatham Rise, and the South African, Californian, East Australian and Peruvian margins generally have both $\delta^{13}C$ and $\Delta^{34}S$ within 2‰ of seawater values (Fig. 9). However, late Pleistocene – Holocene Namibian concretions, Tertiary Sechura Desert and Ica Plateau deposits in Peru, Oligo-Miocene phosphorites from southern Florida, and Upper Cretaceous – Palaeogene Moroccan phosphate grains yield $\delta^{13}C$ of close to –7‰ and $\Delta^{34}S$ up to +10‰. The latter group, therefore, confirm that the $\delta^{13}C$ of "anoxic" francolites is apparently relatively uniform, but $\Delta^{34}S$ varies considerably between high positive and, in one case, low negative values (Fig. 9; Nathan & Nielsen 1980; McArthur et al. 1986; Piper & Kolodny 1987).

Large variation in $\Delta^{34}S$ is not unexpected given the complexity of sulphur isotope systematics, and likely differences in the extent and rate of sulphate reduction and openness of diagenetic systems. Additionally, negative $\Delta^{34}S$ values might in some cases be caused by ^{34}S-depleted H_2S diffusing upwards from an Fe-poor sulphate reducing environment being oxidised to sulphate at the anoxic/ suboxic interface. Similarly, upwards diffusion of CO_2 produced by high rates of organic degradation may promote lower $\delta^{13}C$ values of dissolved inorganic carbon in overlying zones. Francolites precipitated in such condition might be expected to exhibit a light sulphur and carbon signature. A Namibian

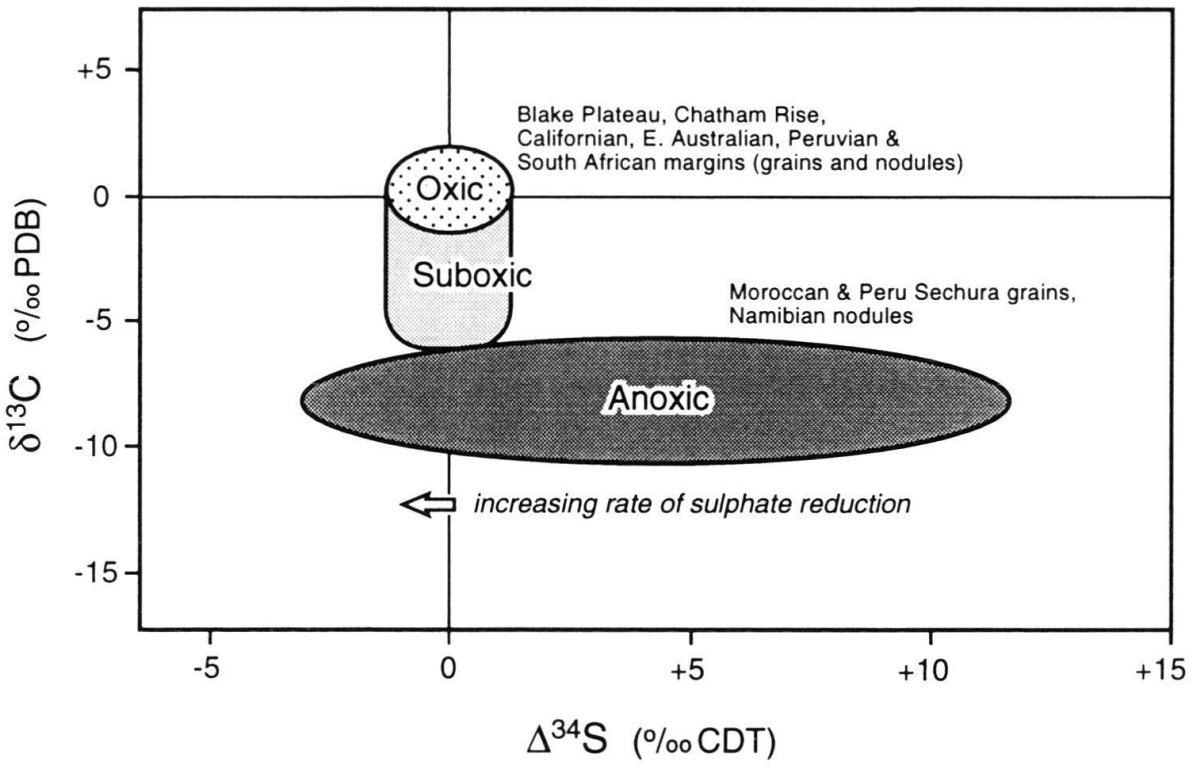

Fig. 9. Variation of $\delta^{34}S$ and $\delta^{13}C$ in modern and ancient francolites. Sulphur isotopes are expressed as $\Delta^{34}S$, calculated as $\delta^{34}S$(francolite) – $\delta^{34}S$ (coeval evaporite), to compensate for secular variation in seawater compositions (modified from McArthur et al. 1986).

concretion studied by McArthur et al. (1986) provides one possible example of precipitation under these conditions, although the negative $\Delta^{34}S$ value might equally be a result of a very high rate of sulphate reduction caused by the abnormally high organic carbon content (up to 26%) of the host sediments.

Sulphur stable-isotopes, therefore, yield valuable information which together with coexisting oxygen and carbon data are able to provide strong constraints on phosphogenic environments. It is interesting to note that results obtained to date indicate that there is no clear relationship between phosphorite type (i.e. nodular versus granular) and diagenetic environment. In both facies, francolite cements precipitate under oxic to suboxic or, less commonly, anoxic conditions. Even in anoxic environments, however, the relatively constant composition of francolites suggests that major ions such as Ca, Mg and Sr are able to diffuse freely from seawater. The possibility that such ions are sourced from dissolving carbonate appears to be inconsistent with Sr-isotope data (see below), which indicate precipitation in equilibrium with contemporary ocean water rather than inheritance of carbonate-derived Sr. Furthermore, many 'anoxic' francolites such as those from Namibia and the Sechura are not associated with carbonate. It seems likely, therefore, that francolite precipitation occurs almost entirely in the uppermost few decimetres of the sediment column.

Strontium isotopes

The residence time of Sr in seawater is about 3 Myr (Richter & Turekian 1993), also several orders of magnitude longer than oceanic mixing times, so the oceans are well-mixed

with respect to Sr. The $^{87}Sr/^{86}Sr$ ratio of modern biogenic marine carbonates and seafloor cements is identical to that of seawater at 0.709175 ± 0.000004 (McArthur et al. 1993a), but the ratio in marine carbonates has varied substantially through time, from values of <0.707 during the Late Permian and Late Jurassic to >0.709 during the Early Cambrian and Quaternary (Peterman et al. 1970; Burke et al. 1982; DePaulo & Ingram 1985; Koepnick et al. 1985; Palmer & Elderfield 1985; Hess et al. 1986; Capo & DePaulo 1990; Kaufman et al. 1993; McArthur et al. 1993a, b; Denison et al. 1994b). Recent reviews include those of Veizer (1989), Stille et al. (1992), McArthur (1994) and Smalley et al. (1994).

The $^{87}Sr/^{86}Sr$ ratio of seawater is controlled largely by two major fluxes: (1) riverine and groundwater input, currently around 0.7119; (2) hydrothermal fluids, resulting from the interaction of seawater with young oceanic crust, with compositions of 0.7030. A smaller diagenetic flux from ocean floor sediments has a ratio of 0.7084, and consequently has far less impact on the overall seawater ratio. Secular variation in strontium isotopes is caused, therefore, by factors such as changes in global climate and eustatic sealevel, mountain-building events, and variation in rates of seafloor spreading. Many authors have argued that high erosion rates associated with major phases of tectonic uplift provide the main forcing mechanism on the Phanerozoic Sr-isotope curve, other fluxes producing only second order variation.

The Sr-isotope curve is particularly well-documented for the Cenozoic. During the last 40 Myr, $^{87}Sr/^{86}Sr$ ratios have become systematically heavier from around 0.7078 during the Eocene to 0.7092 at the present day so, at least within this interval, by measuring the ratio of an unknown sample and referring back to a reference curve (Fig. 10), it is sometimes possible to date the sample to with an accuracy of a few hundred thousand years. The precision of such dates is inversely proportional to the slope of the curve and the curves of different authors also diverge at certain intervals, probably as a result of slight differences in stratigraphic assignments, so data tend to become less precise with increasing age. Nonetheless, strontium isotopes provide a means of dating marine sediments which is far beyond the range of more established methods such as U-series disequilibrium and ^{14}C methods.

The high Sr content of francolite (typically around 2700 $\mu g\ g^{-1}$ when formed) makes the mineral well-suited to Sr-isotope studies. Strontium is incorporated into francolite during precipitation, so in the case of phosphatised limestones strontium-isotopes potentially provides a means of assessing the date of mineralisation as opposed to the age of the host limestone, which may be obtained independently via $^{87}Sr/^{86}Sr$ ratios in calcite (Fig. 10), or palaeontological data. Dating of phosphatised hardground surfaces or individual phosphorite clasts in polymictic conglomerates, such as those commonly recovered off the margins of South Africa, Morocco and Spain, should also be feasible.

The use of $^{87}Sr/^{86}Sr$ ratios to date phosphogenesis necessitates a number of assumptions: (1) early diagenetic porewaters retain seawater Sr-isotope ratios; (2) francolite does not inherit Sr from precursor carbonates; (3) ratios remain unaltered during burial diagenesis. These assumptions seem to be generally valid (McArthur et al. 1990; Compton et al. 1990; Hein et al. 1993; Stille et al. 1994). The $^{87}Sr/^{86}Sr$ ratios of modern francolites are within error of modern marine Sr, while older seafloor phosphorites (Fig. 10) yield independent calcite and francolite dates which are consistent with other geological data. For example, it appears (McArthur et al. 1990; McArthur pers. comm. 1994) that on the Chatham Rise off New Zealand, replacement of Oligocene carbonates (29.8–28.1 Ma)

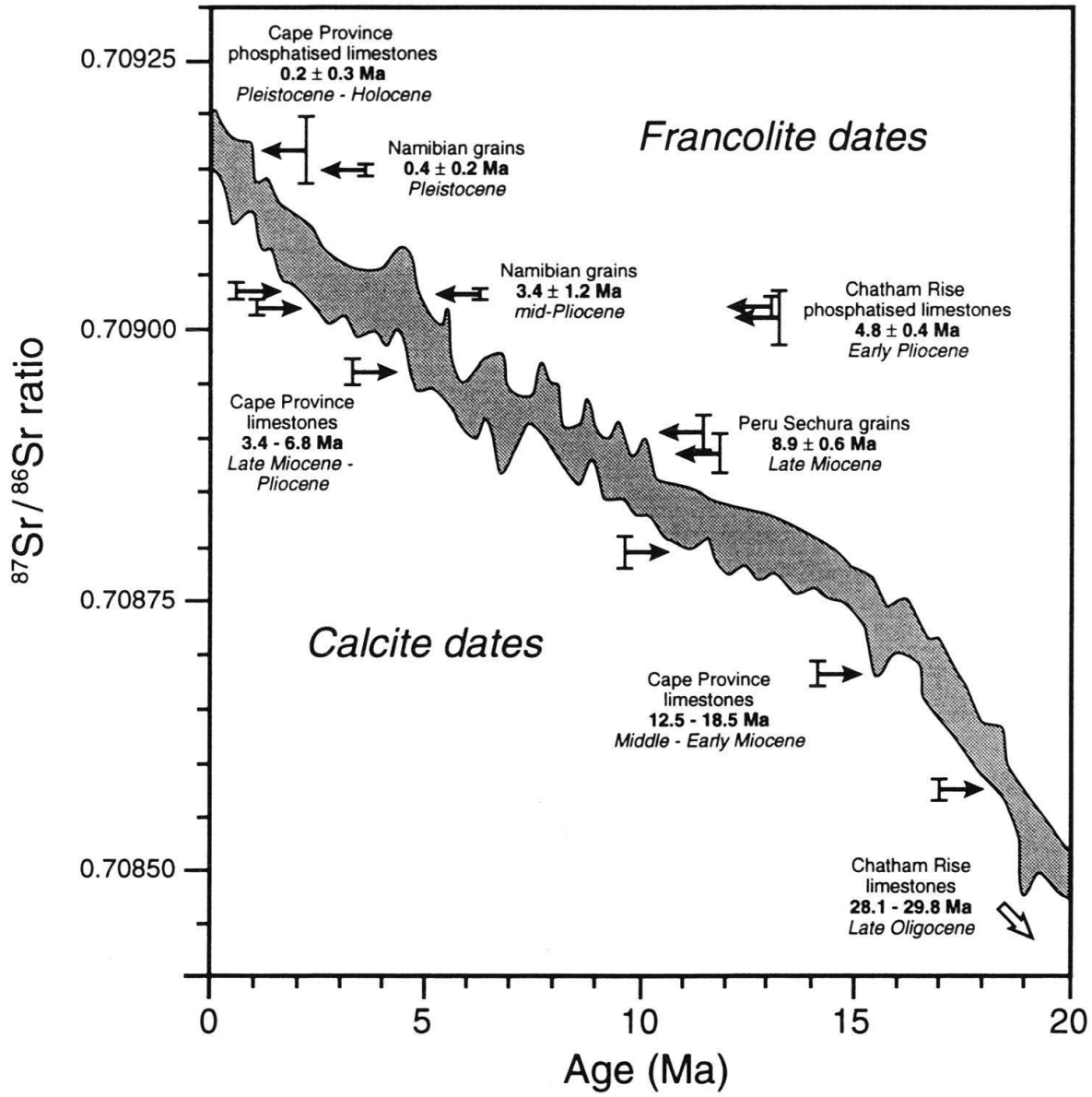

Fig. 10. $^{87}Sr/^{86}Sr$ ratio plotted against age and corresponding dates derived for coexisting francolites (above) and calcites (below) from phosphorites. The stippled area encloses the 95% confidence limit for the Neogene isotope curve of Hodell et al. (1991). Sample data are from McArthur et al. (1990), recalculated for a modern seawater $^{87}Sr/^{86}Sr$ ratio of 0.709175; dates (in part after McArthur pers. comm. 1994) are derived from the regression equations of Hodell et al. (1991). Dating errors were calculated by adding errors on measured $^{87}Sr/^{86}Sr$ ratios to the spread of $^{87}Sr/^{86}Sr$ data defining the isotope curve. Large errors for samples between 4.5–2.5 Ma are caused by the flat nature of the curve over that interval. Note that phosphatisation may post-date limestone deposition by many Myr.

occurred in the Early Pliocene at about 4.8 Ma, Namibian shelf peloidal phosphorites formed in the mid-Pliocene around 3.4 Ma and in the Pleistocene at 0.4 Ma, and the Sechura Desert deposits of Peru are Late Miocene, accumulating around 8.9 Ma. Calcite ages derived from limestones collected off Cape Province South Africa (Fig. 10) range widely from Miocene to Pliocene (18.5–3.4 Ma) but phosphatisation appears to have occurred very recently, during the Pleistocene to Holocene. Errors on these dates are

generally in the order of 0.5 Myr, providing a better resolution than any other suitable dating method currently available.

Similarly, Compton et al. (1993) dated Hawthorn Group phosphorites in southern Florida as early Late Miocene (9.2 ± 1.4 Ma) to Late Oligocene (25.6 ± 0.7 Ma), with a major phosphogenic episode occurring during the Early Miocene between 21.9 and 20.4 Ma. Strontium-derived ages for benthonic foraminifera in sediments surrounding nodules were consistently younger than those obtained from nodule francolites, supporting evidence of extensive reworking. Hein et al. (1993) recognised two major phosphogenic events in the equatorial Pacific at 39–34 Ma (Late Eocene – Early Oligocene) and 27–21 Ma (Late Oligocene – Early Miocene) plus two minor episodes based on Sr-isotope data from seamount phosphorites, although the validity of these particular data has been questioned (McMurtry et al. 1994).

Most recently, Stille et al. (1994) described the Sr-isotope stratigraphy of phosphorites on the North Carolina continental shelf of the US, obtaining Early Miocene ages of 19.3–17.8 Ma. These authors demonstrated that although peloids and brachiopod fragments gave identical ages which are totally consistent with biostratigraphic data, older dates were obtained from coexisting intraclasts (confirming reworking), while vertebrate material yielded younger ages which are consistent with diagenetic modification. Clearly, careful selection of material is essential to obtain a reliable high-resolution isotope stratigraphy from granular phosphorites. Pleistocene and Holocene sediments in the same area yielded peloids with slightly younger Miocene ages (17.24 ± 0.74 Ma), indicating that these grains were derived from a now-eroded part of the phosphorite sequence.

The Sr isotope compositions of ancient apatitic fossils such as conodonts, ichthyoliths, fish teeth and inarticulate brachiopods (Shaw & Wasserburg 1985; Staudigel et al. 1985; Grandjean et al. 1987; Schmitz et al. 1991; Ingram et al. 1994; Stille et al. 1994) are, for the least altered material, in general agreement with the $^{87}Sr/^{86}Sr$ ratio in contemporaneous seawater, although there is a bias towards anomalously high ratios. Trends towards heavier Sr-isotope ratios associated with Sr-loss from francolites during weathering was also observed by McArthur et al. (1987) in their study of meteoric alteration of Lower Pliocene phosphorites from Cape Province, South Africa, so post-depositional exchange can certainly occur.

Clearly, careful screening of samples using a combination of petrographic, trace-element and stable-isotope geochemical techniques (Denison et al. 1994a; McArthur 1994; Smalley et al. 1994) is essential before applying Sr isotopes as a stratigraphic tool. One further note of caution is that many authors have used strong mineral acids to dissolve their samples. Although in most cases relatively pure material was selected, minor contamination of $^{87}Sr/^{86}Sr$ ratios from the siliclastic fraction remains possible, which is liable to induce slightly elevated values (McArthur et al. 1993b), and therefore, in the Tertiary, younger ages. The use of a less aggressive digestion procedure (e.g. McArthur et al. 1990) would clearly be advantageous.

It may be concluded that Sr isotopes provide an excellent method of dating phosphogenesis. Three reservations have still to be made: (1) the Cenozoic $^{87}Sr/^{86}Sr$ seawater-curve is now fairly well-established, but for older sediments determinations are more problematic; even in the Tertiary, some intervals may be dated much less precisely than others due to the low gradient of the curve or to poorer biostratigraphic resolution; (2) multi-generation deposits in which reworking has redistributed phosphorite from several

sources and ages into a single bed are common, so it is important to select the same phosphate grain-type and grain generation to obtain reproducible and reliable ages; (3) different ages than the time of phosphogenesis may be obtained due to alteration or the use of inappropriate dissolution techniques.

Neodymium isotopes

Unlike Sr, the residence time of Nd in the oceans is thought to be in the order of hundreds of years to perhaps 2 kyr (Piepgras et al. 1979; Piepgras & Wasserburg 1980; Jeandel 1993), shorter than or comparable to the ocean mixing time of around 1.5 kyr. Consequently, the distribution of Nd is heterogeneous, with each major ocean basin having a relatively limited and characteristic range of $^{143}Nd/^{144}Nd$ ratios.

The $^{143}Nd/^{144}Nd$ ratio of a sample is a product of the radioactive decay of ^{147}Sm to ^{143}Nd at a constant rate (λ_{Sm}) of 6.54×10^{-12} yr^{-1}, and so reflects both the age and initial $^{147}Sm/^{144}Nd$ ratio. On a global scale, $^{143}Nd/^{144}Nd$ ratios have been increasing steadily since the formation of the Earth at 4.6 Ga. Comparisons between $^{143}Nd/^{144}Nd$ ratios of different samples is strictly only valid, therefore, if all are of the same age. To compensate for these changes, Nd isotopes are generally reported as epsilon (εNd) values (DePaulo & Wasserburg 1976), which incorporate a time factor:

$$\varepsilon Nd(T) = [[(^{143}Nd/^{144}Nd)_{rock,\,T} / (^{143}Nd/^{144}Nd)_{CHUR,\,T}] - 1] \times 10^4 \quad (4)$$

where: $(^{143}Nd/^{144}Nd)_{rock,\,T}$ is the ratio in the sample at time T, and CHUR is a chondritic uniform reservoir (i.e. the bulk earth).

The composition of (CHUR, T) may be calculated (see Rollinson 1993 for a recent detailed exposition):

$$(^{143}Nd/^{144}Nd)_{CHUR,\,T} = (^{143}Nd/^{144}Nd)_{CHUR,\,today} - [(^{147}Sm/^{144}Nd)_{CHUR,\,today} \cdot (\exp(\lambda_{Sm}T) - 1)] \quad (5)$$

Commonly used values for CHUR, *today* are: $^{143}Nd/^{144}Nd = 0.512638$; $^{147}Sm/^{144}Nd = 0.1967$ (Jacobsen & Wasserburg 1980). The initial ratio of the sample (rock, T) may be calculated using the same general equation, but substituting the $^{143}Nd/^{144}Nd$ and $^{147}Sm/^{144}Nd$ ratios measured in the rock for those of CHUR.

Neodymium isotope ratios have been measured in phosphorites by Shaw & Wasserburg (1985), McArthur et al. (1987), Keto & Jacobsen (1988) and Stille et al. (1994), and in biogenic phosphate by a number of workers (Wright et al. 1984; Shaw & Wasserburg 1985; Staudigel et al. 1985; Grandjean et al. 1987; Keto & Jacobsen 1987, 1988). Unfortunately, some of the early work (including that by Shaw & Wasserburg 1985) was undertaken on weathered samples (McArthur pers. comm. 1994) making much of the data unreliable. The εNd values of modern phosphorites and biogenic apatites appear to reflect a time-averaged equivalent of those in seawater, which in the Atlantic (Stille et al. 1992; Bertram & Elderfield 1993) has low $^{143}Nd/^{144}Nd$ ratios (εNd of -12 ± 2), while Pacific waters are higher, with ε values of -3 ± 2, and the Indian Ocean lies in between, around -8 ± 2. These differences reflect the dominant sources of REEs in each ocean basin, from old continental crust in the Atlantic, compared with young crustal and active hydrothermal systems in the Pacific. Smaller differences occur within individual basins (e.g.

Jeandel 1993) and may be used to trace the origins, distribution and evolution of different water masses.

Geochemically distinct water masses seem to have existed in the Atlantic and Pacific for about the last 50 Myr (Fig. 11), prior to which a convergence of εNd values to between –10 and –5 indicates the existence of a single uniform ocean (Panthalassa; Keto & Jacobsen 1987, 1988). Earlier in the geological record, however, there is strong evidence of the existence of separate geochemical provinces. During the Cambrian and Ordovician (Keto & Jacobsen op. cit.), so-called "North Iapetus" rocks from North America have low $^{143}Nd/^{144}Nd$ ratios and εNd values of –20 to –10, while "South Iapetus" material from Europe and the south-eastern US exhibits values around –5 to –9. Only with the onset of the Taconic Orogeny in eastern North America at the end of the Ordovician, did this geochemical separation of water masses in the Iapetus Ocean disappear.

On a smaller scale, an isolated basin in the South Atlantic during the Upper Cretaceous – Palaeocene (Grandjean et al. 1987) is indicated by low εNd values of around –15 in biogenic phosphates (Fig. 11) from the rocks of West Africa (Togo, Guinea, Angola). In some cases samples have $^{87}Sr/^{86}Sr$ ratios of contemporaneous seawater, but εNd values of an isolated basin, indicating good connection with the world ocean but limited short-term mixing. Isolation appears to have continued until the mid-Eocene when a modern oceanic circulation pattern was established. More recently, Stille et al. (1994) demonstrated that francolite $^{143}Nd/^{144}Nd$ ratios are constant in their Miocene phosphorite (peloid) samples and are thought to be representative of western mid-Atlantic (Gulf

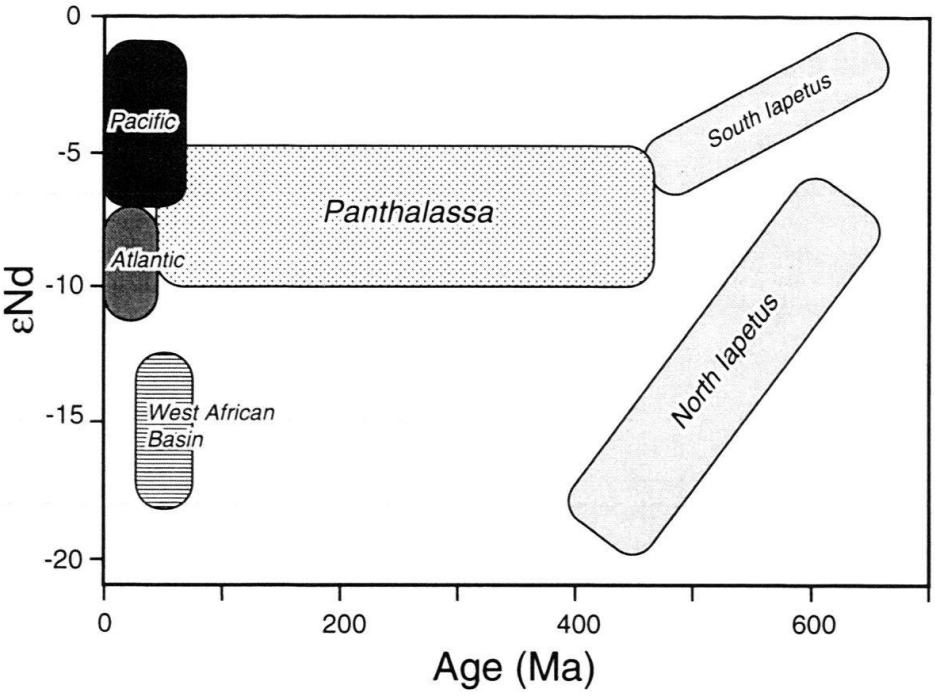

Fig. 11. εNd versus age for Phanerozoic phosphatic fossils. Discrete Atlantic and Pacific provinces are identifiable back to 50 Ma, but data indicate the dominance of a single well-mixed oceanic reservoir (Panthalassa) between 50–450 Ma. A distinct West African Basin water mass existed during the U. Cretaceous – Palaeocene. Prior to 450 Ma, discrete South and North Iapetus water masses may be distinguished (modified from Kolodny & Luz 1992; data from: Shaw & Wasserburg 1985; Staudigel et al. 1985; Grandjean et al. 1987, 1988; Keto & Jacobsen 1987).

Stream) seawater at 19.3–17.8 Ma. However, marginally younger Miocene peloids reworked into Holocene sediments have substantially lower Nd-isotope ratios, suggesting that a major change occurred in oceanic current conditions along the Carolina continental margin around 17.2 Ma.

It is noteworthy that even though there is clear evidence that the REEs, including Nd, are lost from francolite during weathering, relatively intense weathering does not necessarily affect εNd values (McArthur et al. 1987; Stille et al. 1994). Clearly then, Nd isotopes in phosphorites and biogenic phosphates appear to offer a relatively robust and very powerful means of studying water-mass distributions and palaeoceanographic circulation, and may be used to estimate the average age of exposed continental crust bordering ancient ocean basins.

Uranium isotopes

The basis of natural uranium-series dating of phosphorites is the assumption that U is incorporated during phosphogenesis and that ^{230}Th and ^{231}Pa, the radioactive daughters of U, develop in the sample as a function of time according to their half-lives. The residence time of U in the oceans is around 330 kyr (Richter & Turekian 1993), so the modern ocean are isotopically uniform with a $^{234}U/^{238}U$ activity ratio of 1.144 ± 0.004. The use of radiogenic isotopes for dating requires that: (1) U, but little or no Th or Pa, was incorporated into the phosphorite during or very soon after its formation; (2) U is of marine origin with a $^{234}U/^{238}U$ activity ratio close to seawater; (3) the phosphorite has remained closed with respect to U, Th and Pa isotopes. Extensive work over the last 25 years has shown that these assumptions appear to be broadly valid.

Uranium-series dating was fundamental in demonstrating the very limited nature of phosphogenesis in the modern oceans. Prior to the 1970s, it had been assumed (McKelvey et al. 1953; Sheldon 1964; McKelvey, 1967; see Cook et al. 1990 for a historical review) that the widespread occurrence of seafloor phosphorites along the western margins of most continents, provided definitive proof of the link between upwelling and phosphogenesis, as proposed many years earlier by Kazakov (1937). Uranium-series studies of phosphorites from off California, the Chatham Rise and Agulhas Bank by Kolodny (1969) and Kolodny & Kaplan (1970a), however, showed that none of these had an excess of ^{234}U and must be older than 800 ka. It was only later, that studies of deposits off the Peru-Chile and Namibian margins (Baturin et al. 1972, 1974; Veeh et al. 1973, 1974; Burnett & Veeh 1977; Burnett et al. 1980) proved that these contained a $^{234}U/^{238}U$ activity ratio very close to present seawater and must be forming at the present day. Subsequently, other modern phosphorites have been identified off western South Africa (Birch et al. 1983; McArthur et al. 1988) and East Australia (Kress & Veeh, 1980; O'Brien & Veeh 1980; O'Brien et al. 1986, 1990).

Dates obtained from $^{234}U/^{238}U$ activity ratios may be confirmed by comparison with other components of the decay series. The use of "concordia" diagrams for $^{234}U/^{238}U$ (Fig. 12) and $^{231}Pa/^{235}U$ (Fig. 13) versus $^{230}Th/^{234}U$, may be used to test the coherence of the decay series data. Such work has confirmed that the initial $^{234}U/^{238}U$ activity ratio in phosphorites is slightly higher than that in modern seawater, possibly due to the addition of small amounts of ^{234}U to porewaters from the host sediment (Veeh & Burnett 1982). Alternatively, higher ratios might be caused by secular variation in the isotopic composi-

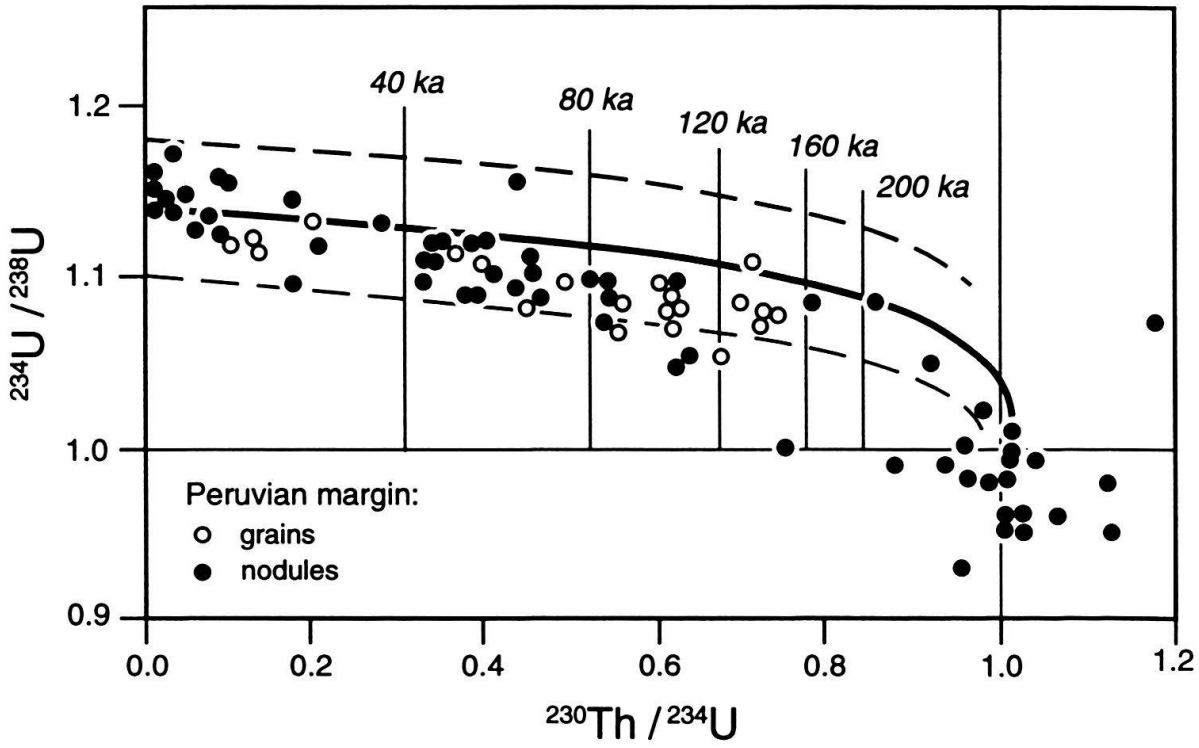

Fig. 12. Ideal development in time or "concordia" (heavy curved line) of $^{234}U/^{238}U$ activity ratios versus $^{230}Th/^{234}U$, with data plotted for Peruvian margin nodules and grains. Note the occurrence of initial $^{234}U/^{238}U$ activity ratios of >1.14, and the occurrence of old nodules with $^{234}U/^{238}U$ ratios of <1.0. The dashed curved lines enclose a deviation of 2σ from the concordia path (data from: Burnett et al. 1988; Burnett & Veeh 1977; Veeh & Burnett 1982).

tion of seawater (Richter & Turekian 1993), although there is no clear evidence that such variation has occurred during the last 200 kyr (Henderson et al. 1993).

The occurrence of old nodules with $^{234}U/^{238}U$ activity ratios of <1 and anomalously low $^{234}U/^{238}U$ versus $^{230}Th/^{234}U$ values (Fig. 12) indicate that decay occurs in a semi-closed system in which a small fraction of ^{234}U is lost to porewaters. Limited isotopic exchange between phosphorites and porewaters in samples from the Peru-Chile Shelf is confirmed by ^{230}Th and ^{231}Pa data (Fig. 13; Veeh 1982; Burnett et al. 1988), but does not invalidate the dating method; samples from the South African (Roe et al. 1982; McArthur et al. 1988) and East Australian (Fig. 13; O'Brien et al. 1986) margins show no evidence of exchange.

Detailed geochronologies of Peru-Chile (Burnett & Veeh 1977) and western South African (McArthur et al. 1988) phosphorite nodules suggest that phosphogenesis is episodic, occurring preferentially during periods of high eustatic sealevel. On the East Australian margin, on the other hand, phosphogenesis appears to have been more or less continuous over the last 180 kyr (Kress & Veeh 1980; O'Brien & Veeh 1980; O'Brien et al. 1986). These differences must relate to the contrasting sedimentological and oceanographic settings of the two areas. It is interesting to note that phosphorite deposition also appears to be episodic on much longer time scales (Cook & McElhinny 1979; Cook 1984; Glenn et al. 1994b).

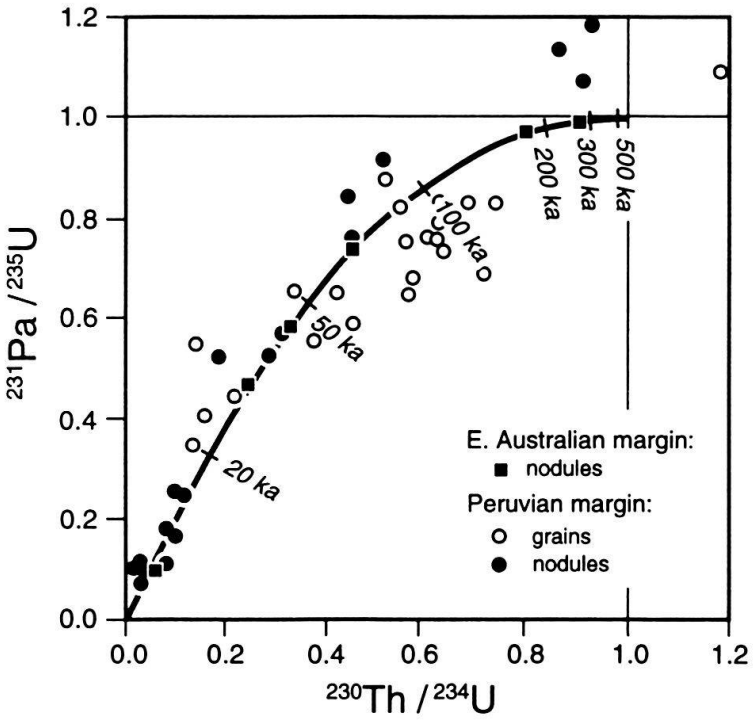

Fig. 13. Concordia diagram of the activity ratios of $^{231}Pa/^{235}U$ versus $^{230}Th/^{234}U$, with data plotted for Peruvian margin nodules and grains, and East Australian margin nodules. Note the concordant ages of nodules from Australia, but the "excess Pa" in the Peruvian nodules and "excess Th" in Peruvian grains (data from: Veeh 1982; Burnett et al. 1982, 1988).

Detailed uranium-series studies of individual grains, nodules and crusts may be used to elucidate the modes and rates of growth of phosphorites. The $^{230}Th/^{234}U$ age profiles of subsamples taken across nodules and crusts (Burnett et al. 1982, 1983; Kim & Burnett 1986) indicate that nodules located at the sediment/water interface grow *downwards* into the soft underlying mud, while buried crusts grow *upwards* within the sediment. This is not surprising given the subsurface nature of the porewater phosphate maximum (Fig. 1, 2). Measured nodule growth rates vary from <0.1–1 cm kyr^{-1}, considerably slower than the surrounding sediments which are accumulating at a rate of at least 2–10 cm kyr^{-1}. The retention of nodules at the sediment/water interface, therefore, must be explained by the buoying action of the burrowing infauna, or perhaps by periods of non-deposition or erosion. Most recently, Burnett et al. (1988) employed a combination of high-precision U-disequilibrium dating with accelerator mass spectrometry (AMS) ^{14}C dating of francoliteCO_2 to show that Peru margin phosphorite grains grow more rapidly than nodules, probably taking < 10 years to become fully developed.

Kolodny & Kaplan (1970a) and later workers (Burnett & Veeh 1977; O'Brien & Veeh 1980; Veeh & Burnett 1982) demonstrated that the $^{234}U/^{238}U$ ratio in phosphorites is affected by U oxidation states, with higher ratios in U(VI) than U(IV). It is suggested that these differences arise during the oxidation of U which causes a small leakage of ^{234}U from U(IV) to U(VI), via the decay of both ^{238}U(IV) and ^{238}U(VI) to ^{234}U(VI). Once in hexavalent state, a small fraction of these ^{234}U atoms may form highly soluble carbonate complexes and diffuse from the phosphorite nodules, resulting in bulk $^{234}U/^{238}U$ ratios which are less than 1.00 in very old samples. Leakage of ^{234}U will introduce a small error into age calculations towards older values. Thus, the outer weathered rims of seafloor phosphorites have lower U(IV) and $^{234}U/^{238}U$(IV) ratios than their unweathered cores (Kolodny & Kaplan 1970a, Baturin & Kochenov 1974).

Using the above principles, O'Brien et al. (1987) demonstrated that East Australian nodules underwent two stages: (1) incorporation of U(IV) under dominantly suboxic conditions in the sediment; (2) oxidation of U to U(VI) during exposure and reworking of the phosphorite on the seafloor. Differences between U(IV) contents and $^{234}U/^{238}U(IV)$ ratios between buried and exposed nodules were related to the length of time nodules were exposed to oxidising conditions at the sediment/water interface. Uranium-series work, therefore, confirms petrographic, sedimentological and other geochemical studies which indicate the importance of reworking in the development of these (and most other) phosphorites.

Environmental issues

On a world-wide basis, the overwhelming majority (>95%) of the 135 Mt of phosphate rock produced annually is used for fertiliser manufacture (Anon 1993). Consequently, long-term growth will ultimately be driven by human population growth, which is expected to remain at current rates for at least several more years (Brown et al. 1987).

In this section, we address some of the most serious problems which effect the environment during the exploitation of phosphate rock. These problems will include those associated with: (1) the mining process; (2) chemical treatments and procedures associated with conversion of phosphate rock to fertiliser; (3) release of toxic or radioactive elements to the environment as a result of mining or processing. In this review, we will emphasise those problems which relate directly to the chemical nature of phosphorites. Many of the current environmental issue centre on contamination by the impurities, especially radionuclides, contained in phosphogypsum, a by-product of fertiliser manufacture, so particular emphasis will be placed on this topic.

Mining and processing

Since most phosphate mining is of the "open-pit" variety, extremely large quantities of material are moved in the process. This type of mining significantly scars the landscape which may not be returned to its original contours following mining. Overburden, ore, ore concentrate, products and by-products are all moved in one form or the other, most often as a slurry which also consumes significant water resources. During the beneficiation process, the ore is concentrated by a variety of methods, usually including sizing and flotation techniques. This results in the production of extremely fine-grained phosphatic "waste clays", one of the most serious environmental problems of the mining/beneficiation part of the fertiliser cycle. This problem is minimised, of course, for deposits (e.g. the Upper Cretaceous – Eocene of the Tethyan province) where the clay content is volumetrically unimportant.

Waste clays are extremely fine grained, with tremendous surface area, so the settling characteristics are very poor. Without any treatment, these clays require decades to settle from about 5 to 20% solids. In Florida, the artificial ponds used for settling take up a substantial (40–60%) fraction of the mine area. Fortunately, progress has been made recently (McFarlin 1992) with rapid dewatering techniques involving the use of a flocculant and floc collector, which brings the solids content up to 25% within a few minutes. Hopefully, this type of technology will prevent the waste clay situation from getting worse in the fu-